# [Proceeding] Collaborative System of Systems Multidisciplinary Design Optimization for Civil Aircraft:AGILE EU project

AIAA AVIATION Forum
5-9 June 2017, Denver, Colorado
18th AIAA/ISSMO Multidisciplinary Analysis and Optimization Conference



# Collaborative System of Systems Multidisciplinary Design Optimization for Civil Aircraft:AGILE EU project

Prajwal Shiva Prakasha[1], Pier Davide Ciampa[1], Luca Boggero [2],Marco Fioriti[2],Benedikt Aigner[3], Artur Mirzoyan[4], Alik Isyanov[4], Kirill Anisimov[5], Innocentiy Kursakov[5] and Andrey Savelyev[5]
*AGILE EU Project, DLR, Blohmstrasse 20 21079 Hamburg*

**As part of H2020 EU project "AGILE", A Collaborative System of Systems Multidisciplinary Design Optimization research approach is presented in this paper. This approach relies on physics-based analysis to evaluate the correlations between the airframe design, as well as propulsion, aircraft systems, aerodynamics, structures and emission, from the early design process, and to exploit the synergies within a simultaneous optimization process. Further, the disciplinary analysis modules from multiple organizations, involved in the optimization are integrated within a distributed framework. The disciplinary analysis tools are not shared, but only the data are distributed among partners through a secured network of framework. In order to enable and to accelerate the deployment of collaborative, large scale design and optimization frameworks, the "AGILE Paradigm", a novel methodology, has been formulated during the project. The main elements composing the AGILE Paradigm are the Knowledge Architecture (KA), and the Collaborative Architecture (CA). The first formalizes the overall product development process in a multi-level structure. The latter formalizes the collaborative process within the entire supply chain, and defines how the multiple stakeholders interact with each other.The current paper is focused on the application of using the AGILE Paradigm to solve system of stystems MDO on a regional jet transport aircraft.**

**The focus of the current research paper is:**

1) **Creation of a system of systems frame work using AGILE Paradigm to support multi-disciplinary distributive analysis capability. The framework involves physics based modules such as : Airframe synthesis, aerodynamics, structures, aircraft systems , propulsion system design, nacelle design, nacelle airframe integration, aircraft mission simulation,costs and emissions.**
2) **Validate the frame work with case study of a regional jet reference aircraft.**
3) **Assess the sensitivity and coupling of design parameters, local disciplinary optimizataion and its effect on global optimization objectives or constraints.**

**The effects of varying Bypass Ratio (BPR) of engine, offtake effects due to degree of electrification and nacelle effects are propagated through the AGILE MDO framework and presented.**



## Nomenclature

| | | |
|---|---|---|
| AGILE | = | **A**ircraft 3rd **G**eneration MDO for **I**nnovative Coll**a**boration of Heterogeneous Teams of **E**xperts |
| ATR | = | Average Temperature Response |
| BPR | = | Bypass Ratio |
| COC | = | Cash Operating Costs |
| CPACS | = | Common Parametric Aircraft Configuration Scheme |
| ED | = | Engine Deck |
| EI | = | Emission Index |

[1] Research Scientist, German Aerospace Center,Blohmstrasse 20 21079 Hamburg, AIAA Member
[2] Researcher, DIMEAS, Politecnico di Torino, C.so Duca degli Abruzzi 24, Torino 10129, AIAA Member
[3] Research Assistant, ILR, RWTH Aachen University, Wuellnerstrasse 7, 52062 Aachen, AIAA Member
[4] Head of Department, CIAM, 2, Aviamotornays Str., Moscow, 111116, AIAA Member
[5] Research Scientist, Propulsion Systems Aero Dept, TsAGI, 1, Zhukovskiy, Moscow Oblast, 140180, AIAA Member

EWT = Electrionic Wind Tunnel
FSMS = Fast and Simple Mission Simulation
GTF = Geared Turbo-Fan
IPCC = Intergovernmental Panel on Climate Change
MDO = Multi Disciplianry Optimization
RC = Recurring Costs
SoS = System of systems
$W_f$ = Fuel flow

# I. Introduction

**Need for Multidisciplinary Design Optimization in Conceptual Design Phase:** Overall Aircraft design and optimization complexity is increasing with stringent environment requirements and demand for improved performance. New technologies are also being developed at faster rate to meet the requirements. The multidisciplinary nature and fragmentation of disciplinary analysis modules make the MDO process complex. As shown in Figure 1, The Blue shade represents conventional situation, red shade represents the need to increase the knowledge and reduce the abstraction level during the conceptual design phase. This reduces the uncertainty and resource overruns in later stage of the design. Thus, there is a need to include multiple disciplinary analysis in the conceptual MDO process.

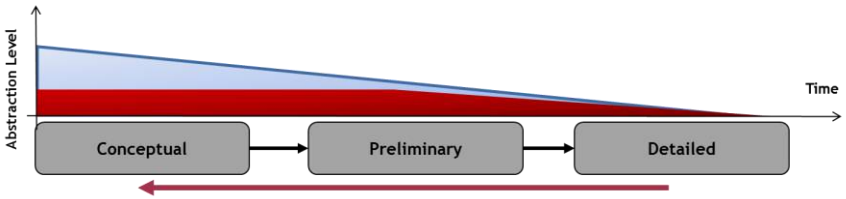


**Figure 1. Aircraft Design Phase and Abstraction levels**

**Need for Collaborative Multidisciplinary Design Optimization:** As the complexity of aircraft design increases, several disciplinary analyses need to be performed. Generally, as the fidelity of the disciplinary analysis increases, the disciplinary expertise does not exist within a single group, and the analysis codes and expertise is spread across several organizations. To solve the challenging complexity of MDO, the distributed competence across organizations need to be brought together within a collaborative frame work, with a standard approach and interface for communication between the disciplinary modules. This requires a new MDO methodologies. Thus, To enable the third generation of MDO, whose challenges are presented in [1], the AGILE Consortium has formulated a novel design methodology,collaborative, large scale design and optimization frameworks, and that in particular (as shown in Figure 2) will:

- Accelerate the setup and the deployment of distributed, cross-organizational MDO processes
- Support the collaborative operation of design systems: integrate specialists and tools
- Exploit the potentials offered by the latest technologies in collaborative design and optimization

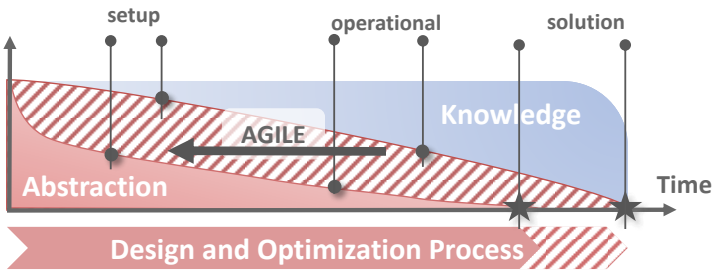


**Figure 2. MDO Paradigm Shift**

## II. Collaborative MDO framework: AGILE Project and the AGILE Paradigm

AGILE Project is an EU initiative to research on Collaborative MDO processes that target significant reductions in aircraft development costs and time to market, leading to cost-effective and greener aircraft solutions. To cope with the challenges of collaborative product development, a team of 19 industry, research and academia partners from Europe, Canada and Russia have joined their efforts.

The overall methodology is introduced in [2]. The implementation of the AGILE Paradigm enables effective collaborative design and optimization of aircraft practiced by heterogeneous design teams, located multi-site, and with distributed expertise. The main elements composing the AGILE Paradigm are the Knowledge Architecture (KA), and the Collaborative Architecture (CA). The first formalizes the overall product development process as a hierarchical layered-structured process. The latter formalizes the collaborative development process, and defines how the multiple stakeholders, acting within each layer of the development process, interface with each other within the entire supply chain. The Collaborative Architecture enables cross-organizational and cross-the-nation integration of distributed design competences of all project partners. The overall AGILE Paradigm is implemented in the so-called AGILE Development Framework (ADF), which defines the overall MDO platform developed in AGILE. The Collaborative Architecture defines the required collaboration elements which need to be deployed to enable effective collaboration within the ADF. The ADF is used for the Collaborative Development Process of aircraft or other complex systems, and can be used to support multiple development stages, such as feasibility studies, conceptual design and/or detailed design. An extensive description on AGILE development process is given in the companion paper I.Gent et al[3], with focus on the AGILE Knowledge Architecture. The Collaborative Architecture aspect is presented in detail in Ciampa et al [4] .**The focus of this paper is on the application of using the AGILE Paradigm, Knowledge and Collaborative Architecture to solve system of systems MDO on a regional jet transport aircraft.**

## III. System of Systems MDO

### A. Overview

The AGILE project is splitted in 3 consecutive Design Campaigns (DC), each one lasting one year, and each one addressing an increasing complexity from use case perspective (progressing from conventional aircraft to novel congurations), and from MDO environment perspective (from the current state-of-the-art MDO system to the 3rd generation system. During DC-1, the reference distributed MDO system has been formulated, and deployed using preliminary design tools and methodologies available in the consortium and applied to the design and optimization of a reference conventional aircraft conguration. The second Design Campaign considered the extension to more complex workows, characterized by high degree of discipline interdependencies, high number of design variables s (see Lefebvre et al[5]). This paper deals with the extension of DC-1 use case , adding more disciplines , higher fidelity tools and exposing more complexity in the coupling, in the objective of performing a system of systems MDO. MDO of System of systems (SoS) in AGILE project is focused on the details of the integration and optimization of the following main disciplinary analysis tools: airframe design, engine, aircraft systems, aerodynamics, structures, nacelle, engine airframe integration, costs and emissions. The MDO systems of systems framework is set up for the analysis and optimization of these disciplines for a given set of requirements.

For a given airframe and mission requirements, several engines with parameters such as Bypass Ratio (BPR), Max Cruise Thrust, Bleed extraction strategies are evaluated in the framework. This engine – airframe optimization is carried out for 4 aircaft system architecures with varying degree of electrification (explained in Section B. 3 below, each system architecture has different Offtake implications on engine and hence fuel consuption). Further is designed based on engine parameters nacelle design and high fidelity engine airframe aerodynamic integaration optimization is performed. With aerodynamics, structural weight, engine performance map'deck, system weight and nacelle drag & weight; mission simulation evaluates the fuel consumption. Emission and cost estimations are carried out for each combination of above mentioned architectures.

The following list comprises the analysis modules of each partner located in different organizations, which are involved in collaborative MDO of SoS:

1) **ED -** Engine Deck, L0-L1 engine simulation model based on the GasTurb v12 commercial tool for engine design and performance simulation (CIAM, Russia)
2) **VAMPzero** - Aircraft synthesis and mission performance model (DLR, Germany)
3) **Aero and Structures** - Aerodynamics and Structural weight module (DLR, Germany)
4) **ASTRID** - On-board systems (OBS) simulation model (PoliTo, Italy)
5) **FSMS -** Fast and Simple Mission simulation (DLR, Germany)

6) **MICADO_costsAndEmissions** - Lifecycle cost and emission simulation model (RWTH Aachen, Germany)
7) **EWT** - Design and local optimization of nacelle geometry/position and HI-Fi optimization of engine airframe integration using EWT solver (TsAGI, Russia)

MDO of SoS is based on the 3 integration/feedback cycles (Figure 3):
**1st Iteration cycle :**Engine Max Thrust and Climb Thrust requirements are matched with Airframe and requirements
**2nd Iteration cycle :** Systems Offtake from Engine , System-Airframe coupling parameters are matched , Systems assumption matching TLAR functional requirements
**MDO Cycle :**Optimization repeats with changing airframe variables (Wing, Fuselage), changing operational performance requirements( Payload and mission). And MDO cycle is performed for each combination of Engine Options and Different Degree of electrification

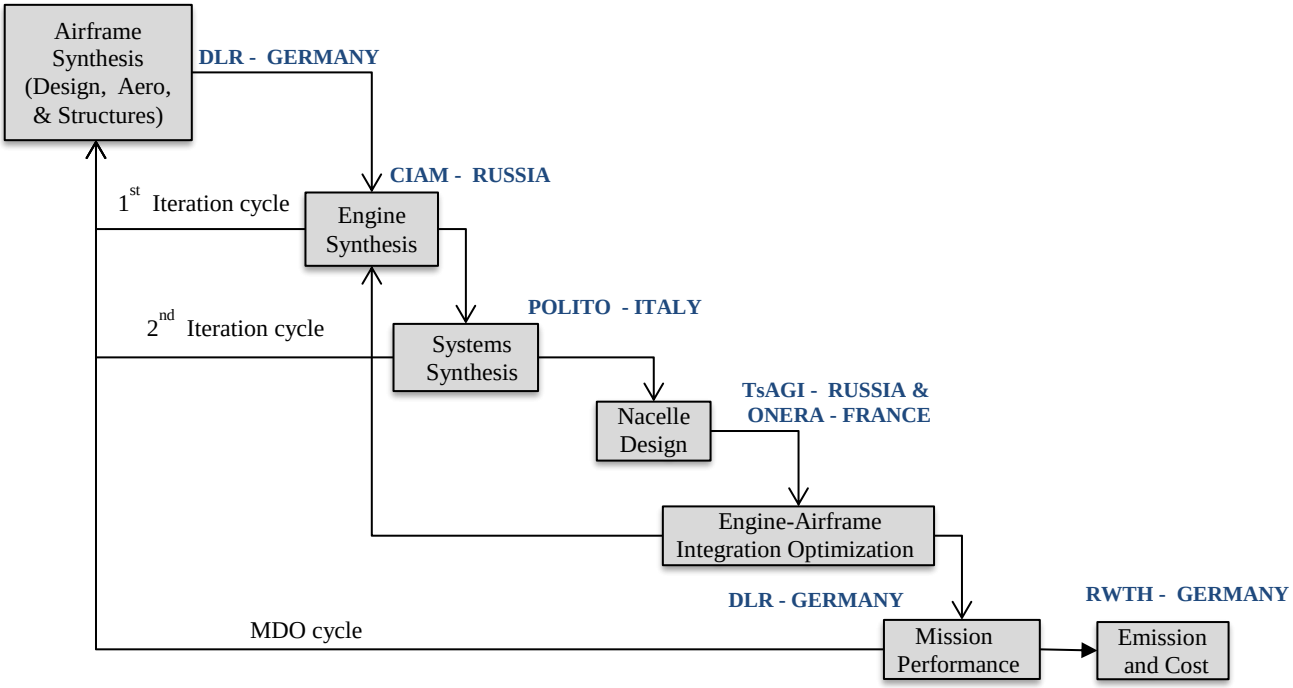


**Figure 3. Systems of Systems MDO Framework**

## B. Disciplinary Module/Competencies

1. *Airframe synthesis including structure and aerodynamics*

The Airframe Synthesis Module consists of a multi-disciplinary, multi-fidelity overall aircraft design system under development at DLR, Germany. The design system is deployed as a decentralized design process, comprising multiple disciplinary analysis and design modules suitable for the pre-design stages. DLR's VAMPzero is an object oriented tool for the conceptual synthesis of aircraft. VAMPzero uses empirical and publicly available aircraft design data and the classical methods available in aircraft design or developed in-house.

**Aerodynamics:** For the current study, a Vortex Lattice Method (VLM) aerodynamics module from DLR, based on the well-known AVL solver, is chosen to calculate the aerodynamics characteristics.

**Structures:** An aeroelastic structural moduleffrom DLR is used for the loads calculation and a FEM based structural sizing of the main structural components. The detailed description or Aero-structural aircraft design can be found in paper by Zill et al. [6] and Ciampa et al.[7]

**Link to other disciplinary modules/tools:** The Aerodynamics Module provides drag polars for structure load analysis as well as to Mission Performance Simulation-to calculate fuel consumption. Structures Module provides airframe winge, fuselage and empennage weights for Aircraft Systems Module and Mission Performance Simulation Module

2. *Propulsion Systems*

Commercial software tools level 1 (L1) for engine modeling were used. Level 1 whole engine simulation tool corresponds engine simulation using 0-level simulation of engine components (compressors, turbines, combustor, etc.), i.e. "black boxes" without detailed (1D-3D) modeling.

Engine analysis module evaluation is based on the operational assumptions, Entry into Service time, engine configuration, power offtake/overboard bleed. The module provides engine installation losses, engine flight envelope, intake pressure recovery description, thrust specifications and engine sizing, thrust reverser ability, engine technical deliveries, engine performance for different operating conditions, engine dimensions description, engine sizing rules, automatic handling of air bleed.

A steady state engine performance is represented by an Engine Deck (ED). The engine deck provides the engine performance for the engine operating envelope (Figure 4). ED for unmixed Geared TurboFan (GTF) with high BPR were provided to AGILE partners.

.

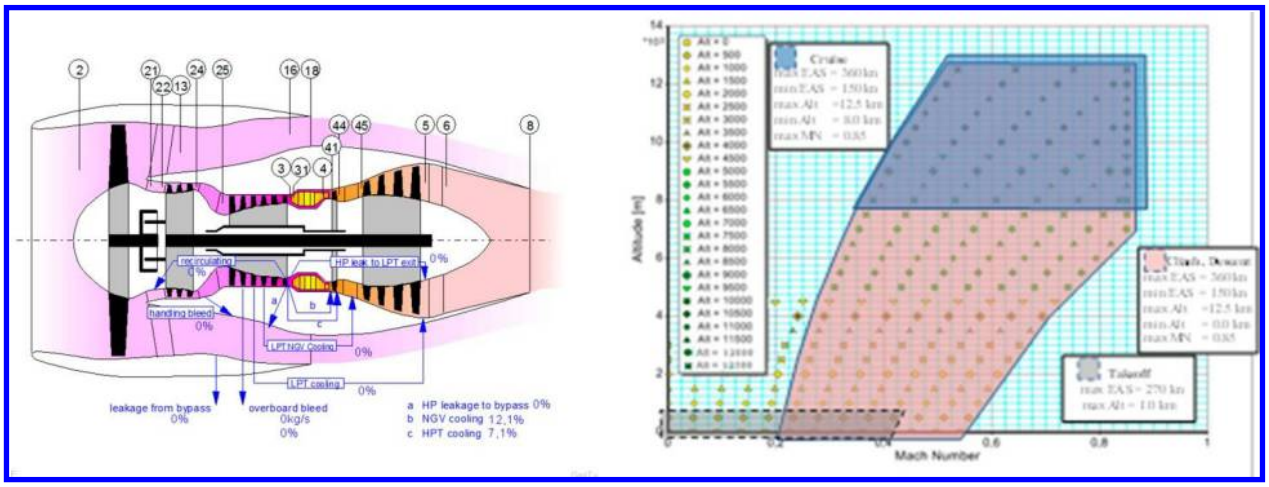


**Figure 4. Engine Stations and flight envelope for different flight segments**

**Link to other disciplinary modules/tools:**The Propulsion System Module provides engine performance map/deck to Mission Simulation Module, Provides engine geometric parameters to Nacelles Design Module and extracts offtake assumptions from Aircraft System Module.

3. *Aircraft Systems (Degree of electrification)*

For aircraft system analysis, ASTRID - Aircraft on-board Systems sizing and TRade-off analysis in Initial Design ,a tool from Politechnico di Torino [8] is used. ASTRID designs power consuming and power generation on-board systems. The formers encompass the avionics, the Flight Control System (FCS), the landing gear, the Wing Ice Protection System (WIPS), the Cowl Ice Protection System (CIPS), the Environmental Control System (ECS), the Auxiliary Power Unit (APU) system, the furnishing and the fuel system. In the latter category, the Electric Power Generation and Distribution System (EPGDS), the Hydraulic Power Generation and Distribution System (HPGDS) and the Pneumatic Power Generation and Distribution System (PPGDS) are considered. The system synthesis tool evaluates the given system architectures and provides power offtakes and bleed air requirement togheter with weight estimation. The power requirement is used by engine module to provide fuel flow for each points in flight envelope for respective bleed and offtake. Moreover, the engine module recalculates the engine specific fuel consumption accordingly with the amount of power offtakes and bleed air required [9].

For current study, four system architectures are evaluated. These four architectures are based on different "Degree of Electrification".

i) **Conventional Architecture CONV :** All actuators use hydraulic technology, the WIPS and the ECS are supplied by high pressure air bleeded by the engine and the electric system generates 115 VAC 400 Hz by Integrated Drive Generators (IDGs), then electric power is converted to 28 VDC (Figure 5 i).

ii) **More Electric Architecture MEA 1:** It derives form the Conventional Architecture, but all actuators are electric, and the electric system generates 235 V AC wild frequency (wf) by alternator. Then electric power is converted to 270 VDC, 115 VAC and 28 VDC (Figure 5 ii).

iii) **More Electric Architecture (Bleedless configuration) MEA 2:** The peculiarity of this architecture is represented by the electrification of the WIPS and the ECS. The wing is indeed protected by heat generated by electrical resistances. The electric system generates 235 V AC wf by alternator and then electric power is converted to 270 VDC, 115 VAC and 28 VDC (Figure 5 iii).

iv) **All Electric Architecture (Bleedless configuration) AEA :** This architecture joints the innovations of MEA 1 and MEA 2. The hydraulic system is removed as all the actuators are moved by high voltage electric power. No bleed air is required, the pneumatic power is produced by dedicated compressors. (Figure 5 iv).

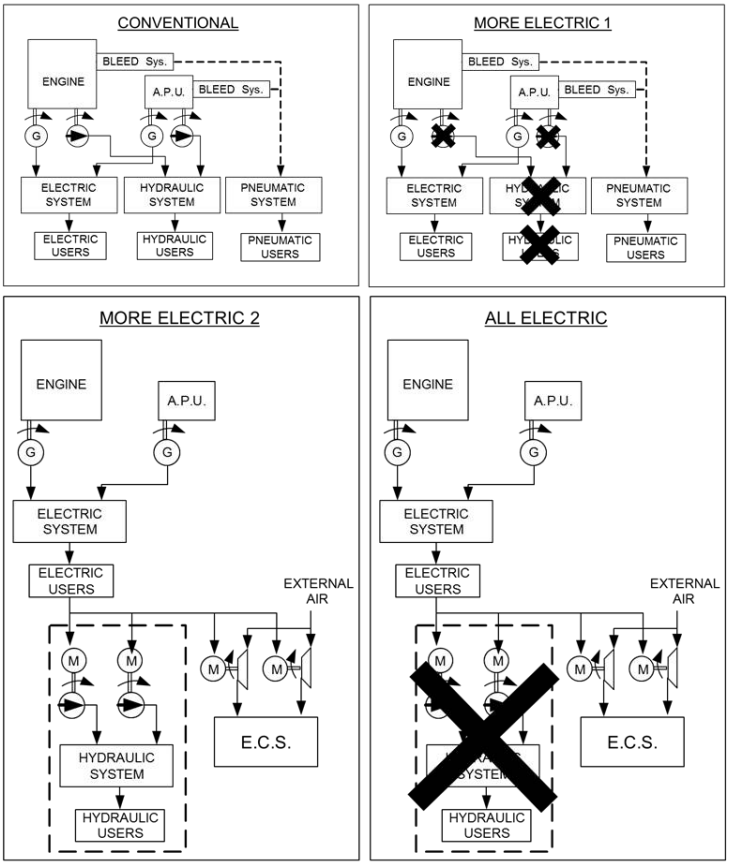


**Figure 5. On-board system Architectures: i) Conventional; ii) More Electric Architecture 1 (MEA 1); iii) More Electric Architecture 2 (MEA 2) and iv) All Electric Architecture (AEA)**

**Link to other disciplinary modules/tools:** The System Synthesis Module extracts information of TLAR,s, Aircraft cabin geometry, aircraft weight parameters and provides system and landing gear weight for final synthesis and Mission Performance Simulation module

4. *Nacelle and Airframe Integration*

The nacelle design and nacelle airframe integration is is divided into two phases. First, Isolated Nacelle Design based on ambient flow, engine geometry and engine gas dynamics properties (Figure 6) and second, engine airframe integration based on the demandance of low installation (Figure 7). For CFD calculations for both phases in-house software Electronic Wind Tunnel (EWT) is used[10]. The Isolated Nacelle Design Optimization is based on 18 geometrical variables. The optimization procedure and features of Isolated Nacelle Optimization prosses is described in Anisimov et al[11].

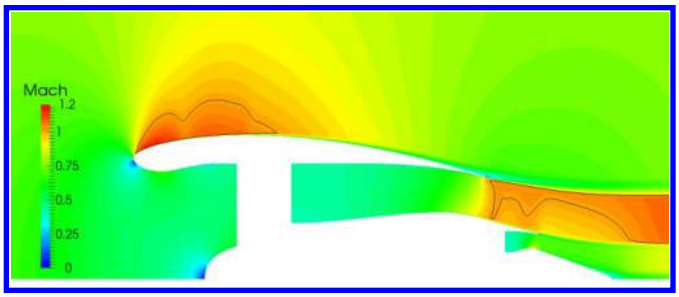


**Figure 6. Nacelle Design Optimization. Mach number field at cruise regime**

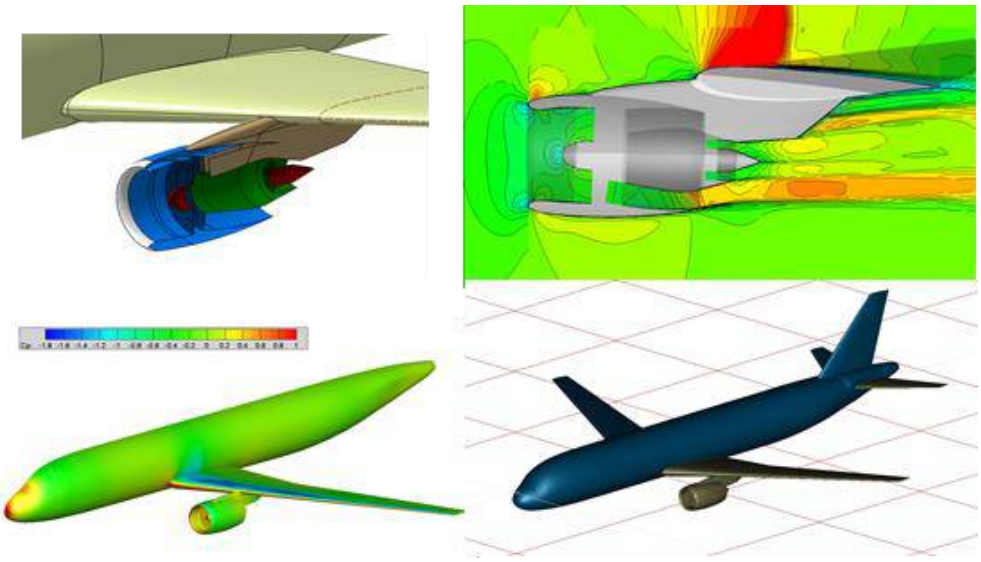

**Figure 7. Nacelle Airframe Integration Optimization (TsAGI)**

Engine Instalation Optimization is based on 5 installation variables. Two installation angles and the three coordinates of the engine displacement have been chosen as independent variable parameters. Engine installation angles: α angle - incidence angle and β - slip angle. The rotation is performed around the lines, which are parallel to Y and Z axes (for α and β, respectively) and pass through the intersection point of the engine axis and the engine entrance plane (the fan plane). The scheme of changes of variable parameters is shown in Figure 8. The optimization technology is the same as for the Isolated Nacelle Optimization.

At each optimization iteration the 3D RANS calculation is done. As a result of solver work, 3D field of the parameters in the cell centers has been obtained. It is necessary to perform the result processing to obtain values of the objective function. As an objective function, the effective losses of engine thrust have been chosen in the current optimization.The Effective thrust is calculated as a sum of the aerodynamic loads on hard surfaces plus the difference between the input and output pulses:

$$P_{eff} = (I_x)_{out} - (I_x)_{out} + \sum (F_x)_{wall}$$

The effective thrust losses are calculated through the ideal thrust (that corresponds to the ideal gas expansion process) and the effective thrust using following formula: $dP_{eff} = \left(1 - \frac{P_{eff}}{P_{ideal}}\right) \cdot 100\,\%$. This value is minimized during the optimization. Since the ideal thrust $P_{ideal}$ and the input and the output pulses is constant from practical point of view, the engine nacelle drag is minimized.

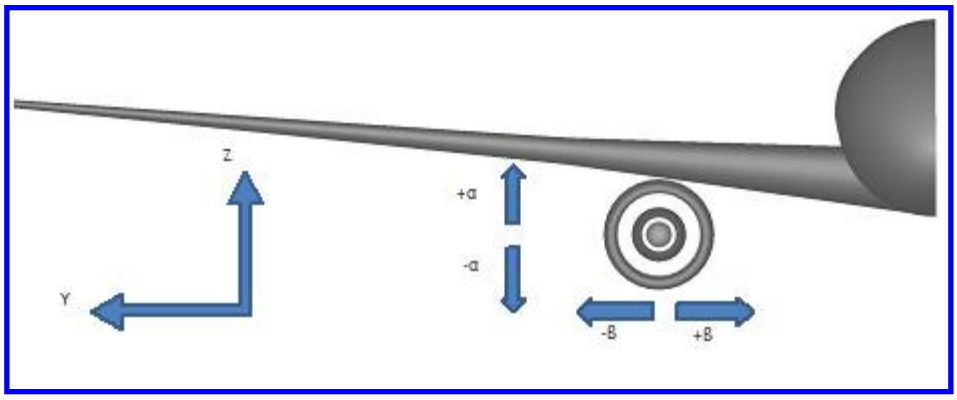


**Figure 8. Rotation angles of the engine**

For optimal positions of each nacelle the pylons have been designed. The procedure of designing the 3D geometric model of the pylon consists of the following steps (Figure 9)

- Developing a framework of 2D cross-sections and guides;
- Creating 3D geometry based on the frame;
- The final modification of pylon geometry: joining the wing and engine nacelle.

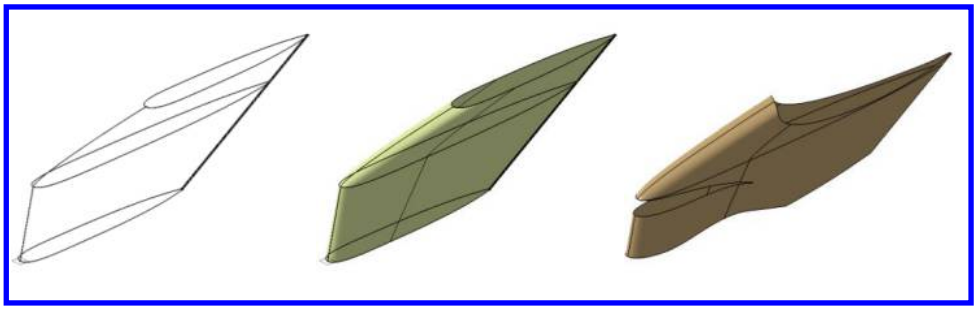

**Figure 9. Stages of the pylon geometry designing**

In accordance with the existing procedure, the pylon is designed after the stages of designing the shape of the wing and engine nacelle. At that, during the variation of the nacelle position under the wing, the pylon geometry is changed. In this connection, the input parameters, which are necessary for the designing the pylon geometry, are the geometric model of the wing, engine nacelle and the engine nacelle position under the wing (in the general case, three spatial coordinates and three angle).

**Link to other disciplinary modules/tools:** Nacelle and Engine Airframe Integration Module extracts information from Aircraft Geometry, Aerodynamics Module, Engine parameters from Engine Module, Offtakes from Aircaft Systems Module and provides optimum Nacelle design to calculate weight and integrated Nacelle Drag. This information is used by Misssion Performance Simulation to evaluate fuel consumption for given mission

5. *Mission Performance Simulation*

The DLR's Mission performance module evaluates the aircraft performance by simulating the given mission phases.The block fuel consumption for given mission and reserve segments are calculated, The FSMS tool uses the drag polars from aerodynamics module, structural weight from structures module, engine deck/engine performance map for analysis. Also the systems weight, Engine weight and Nacelle drag is propagated through Mission simulation to calculate the overall effect of Engine, systems and nacelle on Airframe.

The Typlical Mission for AGILE Reference Aircratf is as per Figure 10 below. 3500 km range (Cruise Altitude = 11000m and Cruise Mach = 0.78) in addition reserve mission of 370 Km (Cruise Altitude = 3000m and Cruise Mach = 0.7). The Mission is constant altitude mission and can also be changed to constant CL and many other parametric variations can be made.

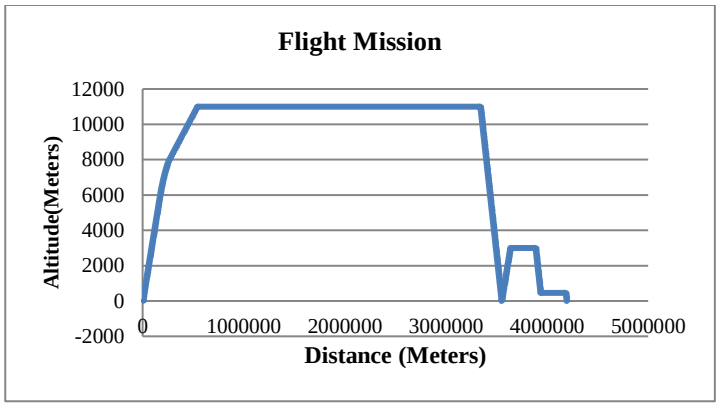


**Figure 10 : AGILE Reference Aircraft Mission**

Figure 11 provides more information of Aircraft Status and Flight Mission parameters along the mission

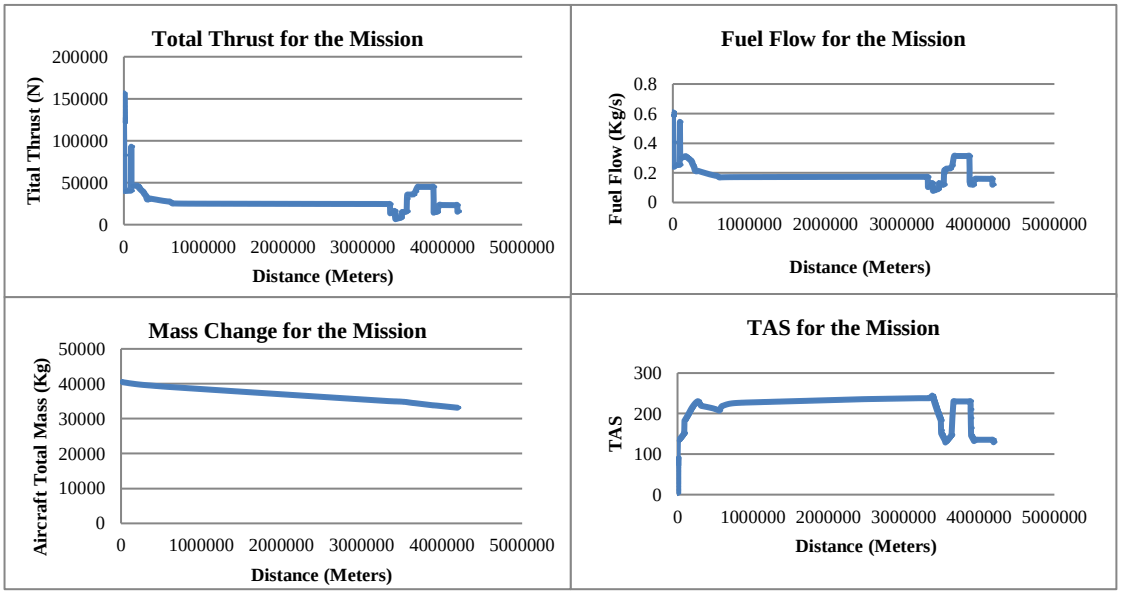


**Figure 11. Flight Mission Parameters Results from Mission Simulation Module**

**Link to other disciplinary modules/tools :** This tool extracts Aero , Weight and Engine Parameters from all the above modules to calculate Mission Fuel. Also links with Cost and Emission Analysis Module for emission and cost modeling.

## 6. *Cost and Emission Analysis*

The cost and emission analysis tools of RWTH Aachen University have been developed at the Institute of Aerospace Systems over the last years and can be used for economic and ecological life cycle assessment of commercial transport aircraft. For the purpose of the studies carried out within the scope of this paper, the focus is set on the production and operational phase, since these are considered to reveal the most significant changes with regard to costs and emissions.

**Costs**: RWTH Aachen's cost module comprises both, non-recurring and recurring costs for an aircraft's life cycle using semi-empirical methods. For non-recurring costs, the methods include for instance costs for development, testing and test facilities, as well as assembly and transport of materials. Operating costs include indirect (administration, staff, etc.) and direct (charges, fees, maintenance, etc.) operational costs of an airline. The concept and sensitivities of the cost analysis tools are described in two research papers by Franz et al.[12] and Lammering et al.[13]

**Emission**: In the performed analysis, the RWTH Aachen emissions module was used to obtain the emission levels of several emissions with regard to the parameter $DP/F00_{x,i}$. This is the ICAO regulatory parameter for

gaseous emissions, expressed as the mass of the pollutant emitted for one incremental step divided by the rated thrust (maximum take-off thrust) of the engine. The total amount of mass for each emission part is then calculated by integration over the whole mission time. For each time step $DP/F00_{x,i}$ is calculated by

$$DP/F_{00_{x,i}} = \frac{EI_i \cdot W_{f,i} \cdot t_i}{F_{00}}, \quad \text{(eq. 1)}$$

Where $i = 1, \ldots, n$ is the index of the current incremental mission step,
$x$ is the emission part (e.g. CO, $CO_2$, $NO_x$, etc.),
$DP/F00_{x,i}$ is the ICAO regulatory parameter for gaseous emissions,
$EI_x$ is the emission index at the current mission step in g per kg of fuel [g/kg],
$W_{f,i}$ is the current fuel flow,
$t_i$ is the time interval of the current mission step,
$F_{00}$ is maximum rated takeoff thrust in kN.

The emission indices $EI_x$ are calculated differently for each emission part. For the analysis carried out in paper it was not possible to obtain all relevant emission parts, due to limitations of the tools used. The emission parts accounted for in this study are $NO_x$, $CO_2$, $H_2O$, $SO_2$ and soot. The emission index for $NO_x$ was obtained by using the engine performance information at all operating conditions given by CIAM. The indices for $CO_2$ and $H_2O$ are stoichiometric factors of the combustion and can therefore be considered as constant values. The emission indices for Sulfur Dioxide ($SO_2$) and soot are also considered to be constant for this study and were obtained from a report of the Intergovernmental Panel on Climate Change (IPCC) from 1999. The values for the three above mentioned emission parts are given in Table 1.

**Table 1. Emission indices[14].**

| Species | Emission index ($EI_x$) |
|---|---|
| $CO_2$ | 3.16 kg/kg fuel |
| $H_2O$ | 1.26 kg/kg fuel |
| $SO_2$ | 0.0002 kg/kg fuel |
| Soot | 0.0004 kg/kg fuel |

The information about the amount of emitted pollutants at each incremental flight step and the additional information about the current flight altitude are processed to an implemented climate model, which was introduced by Dallara[15] in 2010. With the help of this model it is possible to account for the actual ecological effects of the pollutant emissions – such as Average Temperature Response (ATR), or Absolute Global Warming Potential (AGWP) – rather than only considering the pure amount of emitted pollutants. The above described methods of the RWTH Aachen emissions module are also further explained in a publication by Franz et al.[16]

**Link to other disciplinary modules/tools**: Within the scope of the presented SoS MDO use case, the interfaces between the RWTH Aachen modules (*MICADO_CostsAndEmissions*) are twofold. On the one hand, the cost analysis mainly requires information about component sizes, masses, materials, etc. in order to calculate the manufacturing costs. For operational costs characteristic values of interest are e.g. flight duration, frequency, and fuel consumption are additionally required. On the other hand, for the emission assessment, the specified flight mission has to be simulated with focus on exhaust emissions and the respective altitudes at which they are emitted. Therefore, the entire performance mission simulation results at all incremental flight steps are taken as an input for the analysis.

## IV. Reference Aircraft Test Case description and MDO Formulation

### A. Test Case

To evaluate the frame work, a test case of regional Civil Aircraft is considered (Figure 12). A 2020 Entry into Service specification, conventional single aisle, engine under the wing configuration. The TLAR of the Reference test configuration is provided in Table 2.

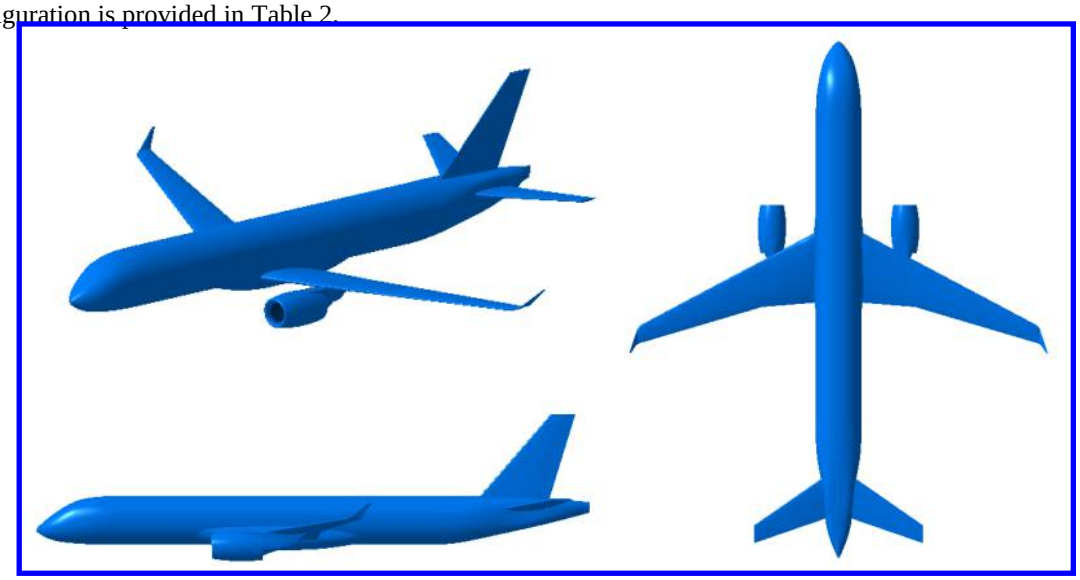

**Figure 12. AGILE reference test case configuration for systems of systems MDO**

**Table 2. TLAR's AGILE Reference Aircraft DC-1**

| Specification | Metric | Imperial |
|---|---|---|
| Range | 3500 km | 1890 nm |
| Design payload | 9180 kg | 20220 lbs |
| Max. payload | 11500 kg | 25330 lbs |
| PAX | 90 pax @ 102 kg | 90 pax @ 225 lbs |
| MLW (% MTOW) | 90% | |
| Long Range Cruise Mach (LRC) | 0.78 | 0.78 |
| Initial Climb Altitude (ICA) | 11000 m | 36000 ft |
| Maximum Operating Altitude | 12500 m | 41000 ft |
| Residual climb rate | 91 m/min | 300 ft/min |
| TOFL (ISA, SL, MTOW) | 1500 m | 4921 ft |
| Vref (ISA, SL, MLW) | < 130 kts | |
| Max. operation speed ($V_{mo}$ / $M_{mo}$) | 330 KCAS / 0.82 | |
| Dive Mach number ($M_d$) | 0.89 | |
| Fuselage diameter | 3 m | 118 in |
| Fuselage length | 34 m | 111.5 ft |
| Service life | 80,000 cycles | |
| Fuel reserves | 5% | 100 nm |
| A/C configuration | Low-wing, wing-mounted engines | |
| Engine | Provided (e.g.: PW1700G) | |
| Design objective | Minimize COC (alternatively, min. MTOW) | |

## B. Sensitivity and MDO Formulation

The diciplines mentioned in Section III were used to formulate a workflow as shown in Figure 13 . The workflow as shown connects the multiple disciplinary competencies hosted by partners in different locations. As per Figure 3 the reference aircraft is analysed and processed by different dicplinary competencies. The analysis results and effects are mitigated through the workflow: For a fixed Airframe (Wing Area and Airframe Geometry) , the Engine BPR change will impact the engine weight and Degree of electrification of aircraft systems will impact the offtake and hence engine performance, there effects are propagated along with weights and Nacelle drag, thus the mission simulation will compute the fuel consumption with propagated effects.

**Objectives:** The formulation is to solve Multi objective optimization problem,minimizing 5 objectives such as

i) Fuel efficiency, fuel consumption at 3500 km range : Primary Objective
ii) Cost criteria, Cash Operating Cost – COC
iii) Emission criteria, LTO emission level – DP/F00 and Average Temperature Response (ATR)

**Assumption:** Initial aircraft is given reference aircraft (including reference airframe, engine, OBS, nacelle geometry/position).Engine size is defined during mission performance calculation using engine modeling by takeoff static net thrust FN00

i) Basic engine size for all engine decks is engine static thrust FN00 = 78.5 kN
ii) 4 basic OBS architecture options are considered: 1 conventional, 2 – more electrical and 1 – all electrical architecture

**Design Variables:** Following 32 parameters were considered as discrete and continious variable for MDO:

i) Airframe - Wing aspect ratio and area (Initially fixed)
ii) Engine - BPR - 3 Bypass Ratio variables and engine setting combinations
iii) Aircraft Systems - 4 discrete variables for levels of DE - Degree of Electrification
iv) Nacelle Design - 18 variables for Nacelle geometry and 5 Nacelle position variables wrt airframe

**MDO Global Constraints:**

i) Range (3500 km)
ii) Takeoff field length TOFL (1500 m)
iii) Engine max diameter (installation limitation due to under wing engine location)

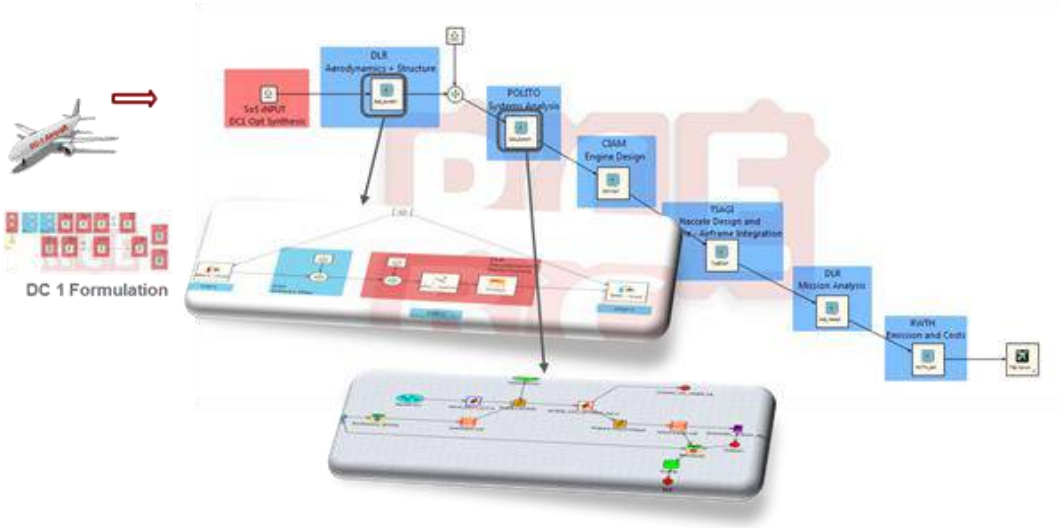


**Figure 13. Sensitivity Study Formulation Framework implemented in RCE**

In the sensitivity studies carried out to this point, the frameworks operates well and the time for execution of each analysis is noted and will be compared with advanced MDO methods using RSM etc (to be presented in conference). Disciplinary results are presented in the paper and for MDO the airframe variables are to be released, results to be updated during the conference.The sensitivity results are presesented in next section.This proves that the framework works for multidicipinary collaboration.

## V. Disciplinary Results, Sensitivity Evaluation and discussion

### A. Disciplinary Optimization Results

Preliminary results of individual disciplines are presented in this section. This result is based on collaborative framework of system of systems evaluation. The impacts of individual discplines are mitigated through the workflow.

1. *Aero Structural Design Module*

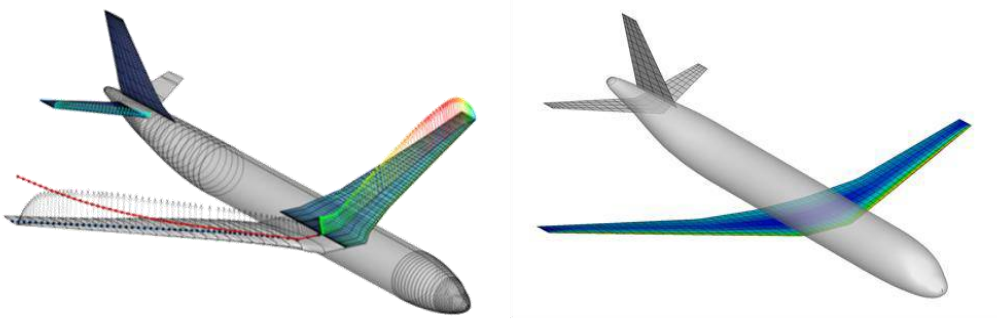

**Figure 14. Notional Aero Structural Design Module Results**

Aerodynamic analysis is performed for each airframe design point. Also, these aerodynamic parameters are used for mission simulation. The aerodynamic loads are considered for structural mass estimation. Certification criteriea of loads are considered for mass estimation of the wing. The following mass chart includes wing mass, empennage mass, engine mass, fuselage mass, nacelle & pylon mass, system & landing gear mass for each BPR and system architecture combination.

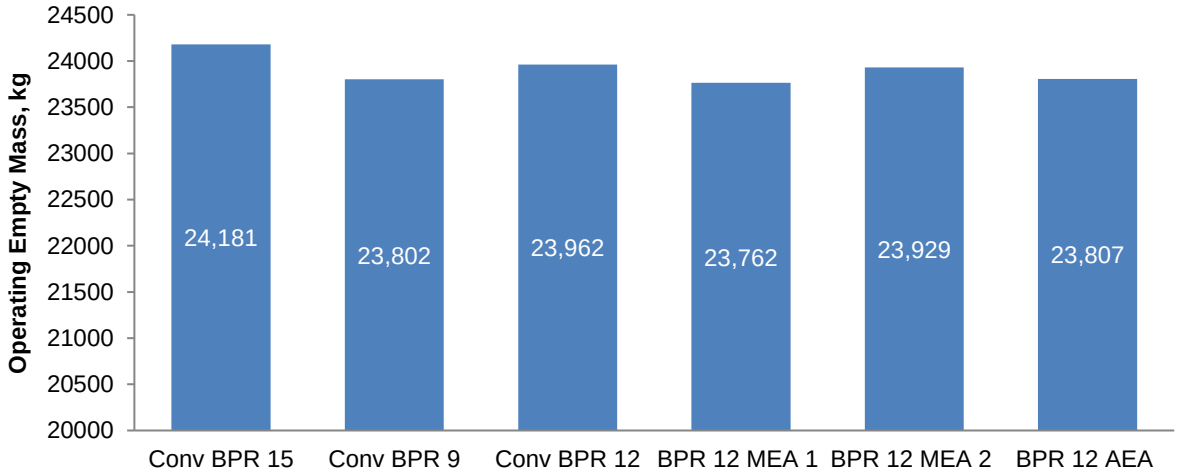


**Figure 15. Operating Empty Mass of AGILE configurations**

2. *Engine Module*

Engine cycle parameters (such as BPR, Overall Pressure Ratio - OPR, Fan Pressure Ratio - FPR, etc.) and engine size are optimized and defined during Engine /Aircraft matching process.

For the activities only BPR was adopted as global design variable. Other engine cycle parameters were defined based on the prototype engine parameters and local engine cycle optimization.

Figure 16 presents the relative levels of the installed Specific Fuel Consumtion (SFC) at Maximum Cruise (MCR) engine rating and M=0.78 and Flight Level FL=11000 m for GTF with BPR 9, 12 and 15, and conventional, MEA1, MEA2 and FEA OBS.

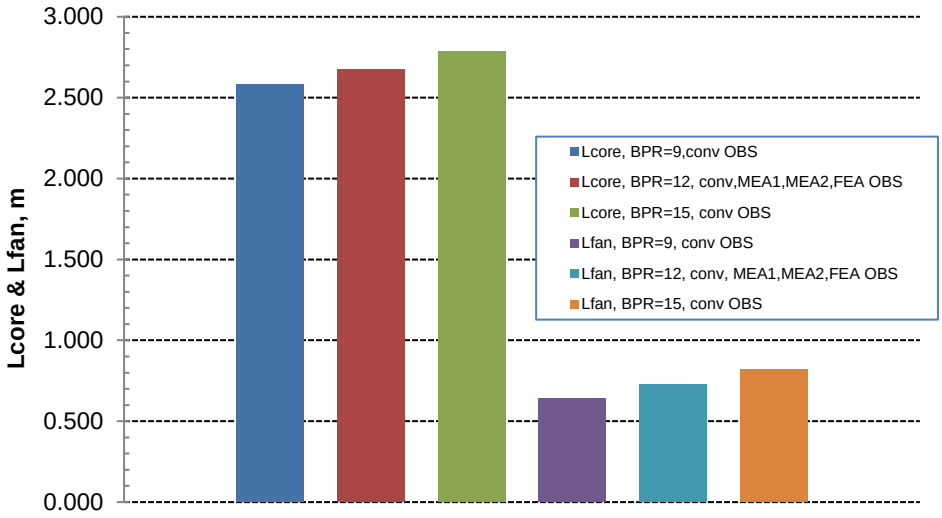


**Figure 16. Installed SFC at Maximum Cruise (MCR) engine rating and M=0.78 and FL=11000 m for GTF with BPR 9, 12 and 15, and conventional, MEA1, MEA2 and FEA OBS**

As expected, SFC at fix maximum cruise thrust is improved with increasing BPR. At the same time, low improvement of engine fuel efficiency due to electrification of OBS is observed. This is due to the fact that a final impact of the degree of aircraft electrification DE through changing of power/air bleed on installed SFC level depends on many factors defining the electrification conditions such as behaviour of engine control system, engine constraints, change of the required cruise engine thrust. Figure 17 shows engine parameters for LTO NOx emission level calculation (GTF with BPR12 and conventional OBS) in the view of Fuel Flow FF and NOx emission index EINOx vs. relative engine thrust rating.

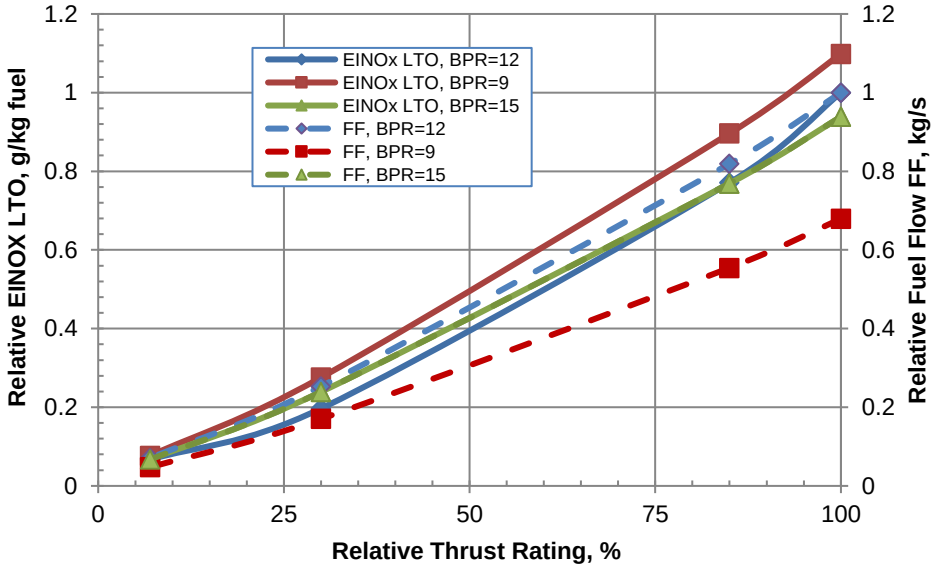


**Figure 17. Relative Fuel Flow FF and NOx emission index EINOx vs. relative engine thrust rating in test rig conditions for GTF with BPR 9, 12 and 15.**

It should be noted that EINOx improvement with increasing of BPR is the result of a decrease of SFC (Fuel flow FF). Figure 18 presents the relative Engine Dry Masses (EDM) for GTF with BPR 9, 12 and 15, and conventional, MEA1, MEA2 and AEA OBS

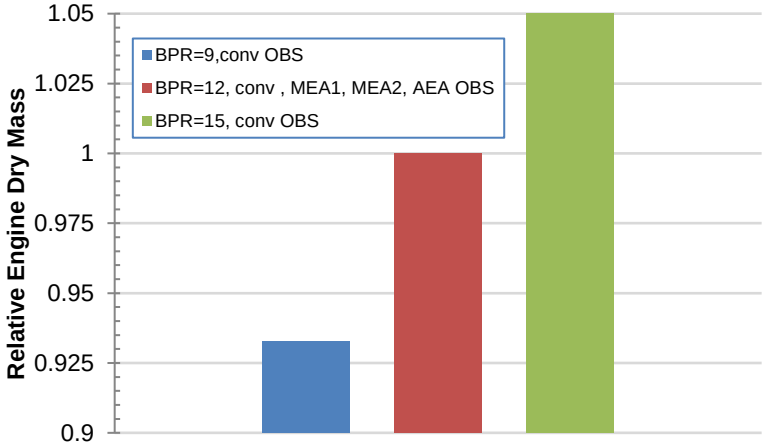


**Figure 18. Relative Engine Dry Mass of GTF with BPR 9, 12 and 15 and conventional, MEA1, MEA2 and AEA aircraft system architecture.**

Increase of EDM with a rise of BPR is mostly connected with the increase of weight of some engine components (fan, IPC, gearbox, etc.). It is understandable that degree of electrification of Aircraft system will have influence on EDM, but due to the complexity of the influence, it was not taken into account in the phase. Figure 19 presents the engine core length $L_{core}$, fan length $L_{fan}$ and engine fan diameter $D_{fan}$ for GTF with BPR 9, 12 and 15, and conventional, MEA1, MEA2 and AEA OBS.

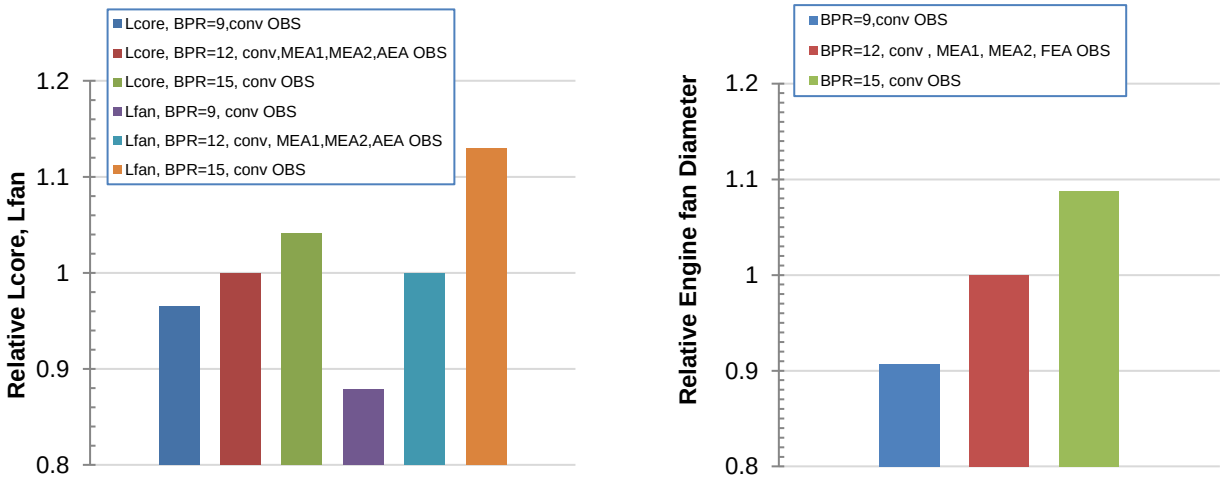


**i)** Relative Engine core length Lcore and engine fan length Lfan

**ii)** Relative engine fan diameter $D_{fan}$

**Figure 19. Engine dimensions for GTF with BPR9, 12, and 15, and conventional, MEA1, MEA2, and AEA OBS**

## 3. *Aircraft System*

Starting from inputs given by propulsion, aerodynamics and overall aircraft design disciplines and including other systems specific inputs, aircraft system design module ASTRID [8] estimates the systems weight and their

power consumption. The weight estimated includes all subsystems and landing gear. Focusing on the weight, as shown in Figure 20, the lightest architectures is the MEA 1 (More electric, first configuration) and the AEA (All electric). In both architectures, all hydraulic users and power generation and distribution are replaced with electrical one. MEA 2 (More electric, second configuration) and the conventional architecture both rely on hydraulic system and the drawback is a notable increment of weight.

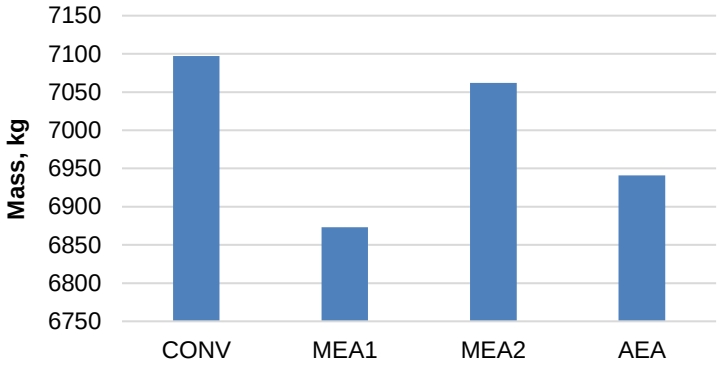


**Figure 20. Weight estimation for the selected on-board systems architectures**

In more details, as shown in Figure 21, the reason of the weight difference among the architectures is not the presence of the hydraulic system only. It is worth noting that the FCS that uses hydraulic technology is lighter than the electric one. However, the weight of hydraulic power distribution and generation reverses this initial advantage. The pneumatic power generated by using dedicated electric driven compressors gives an additional save in weight for MEA2 and AEA configurations. Conversely, as seen for hydraulic technology, the architectures, which rely almost totally on electric technology, faced an increment of the EPGDS. However, this increment in weight is well compensated by the weight saved due to the removal of hydraulic system.

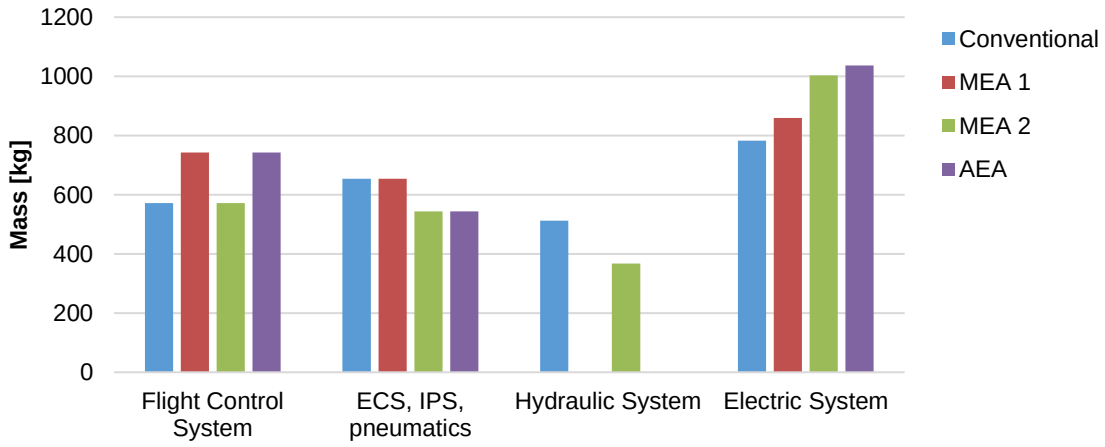


**Figure 21. Weight breakdown of the selected on-board systems architectures**

Regarding the offtakes results, the bleed and the shaft power offtakes during the mission are depicted respectively in Figure 21 and Figure 22. The aircraft mission profile is defined considering systems usage. The bleed air offtake is zero for bleedless architectures, i.e. MEA 2 and AEA since these OBS options rely on dedicated compressors electrically driven Concerning the Conventional Architecture and MEA 1, the bleed airflows reaches its minimum during the cruise segment, since at cruise altitude the anti-ice generally is not required. During taxi phase the bleed air is generally not required by IPS and the air flow needed is relatively low.

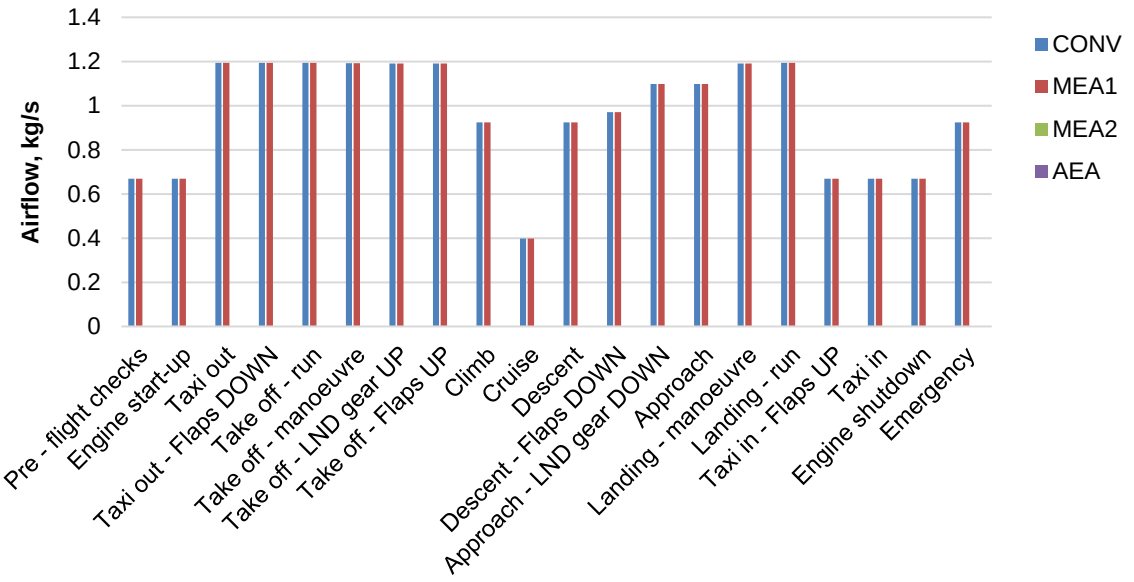


**Figure 22. Bleed offtakes during the mission profile**

The total shaft power represented in Figure 23 is given by the sum of the mechanical powers needed by the electric generators and the hydraulic pumps. It is worth noting that the electrification of the air conditioning and anti-ice systems entails an increment of the shaft power offtakes. However, the equivalent power (i.e. the sum of the power offtakes and the power required to obtain the air flow of compressed air) is lower firstly for AEA and secondly for MEA2 than MEA1 and conventional systems architectures in every phase of the mission profile.[14] For all configurations the power offtakes increment is due to secondary control surface and landing gear extraction. During taxi phase the majority of users are inactive or require low power. The AEA and MEA2 require the greatest power offtakes during climb, cruise and descent phases. It is due to the growing of power required by electrical pressurization system.

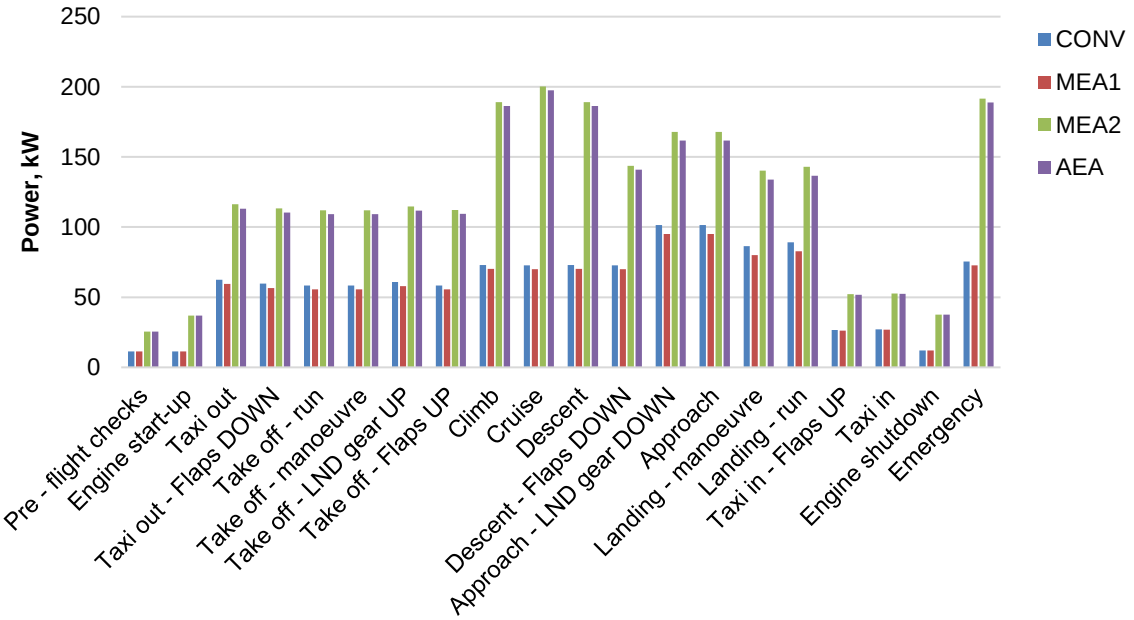


**Figure 23. Shaft power offtakes during the mission profile**

4. *Nacelle Optimization and Engine Airframe Aerodynamic Integration*

This section presents the results for the optimal designing the engine nacelle for 5 turbofan engines. Cruise flight regime at the height H=11000 m with Mach number M=0.78 is considered for optimization configuration. Engine nacelles for 5 variants of turbofan engines are designed:

- turbofan engine of conventional configuration with bypass ratio BPR=9 and takeoff thrust FN00=78.2 kN
- turbofan engine of conventional configuration with bypass ratio BPR =12 and takeoff thrust FN00=78.2 kN
- turbofan engine of conventional configuration with bypass ratio BPR=15 and takeoff thrust FN00=78.2 kN
- turbofan engine of conventional configuration with bypass ratio BPR=12 and takeoff thrust FN00=78.2 kN;
- turbofan engine for Full electric aircraft with bypass ratio BPR=12 and takeoff thrust FN00=78.2 kN;

Three engines with different bypass ratio (BPR = 9, 12 and 15), the engine with BPR = 12 and with extra thrust and the engine with BPR = 12 for full electric aircraft have been considered. The last variant of the engine is characterized by the leak absence of power and air for the internal systems of the aircraft. Input parameters that describe the turbofan engines geometry and gas dynamics are different for each above engine. They and are shown in Table 3.

**Table 3. Geometrical and gas dynamic parameters of considered engines**

| **Parameter** | **BPR=9.0, FN00=78.2 кN, conventional systems** | **BPR=12.0, FN00=78.2 кN, conventional systems** | **BPR=15.0, FN00=78.2 кN, conventional systems** | **BPR=12.0, FN00=90.0 кN, conventional systems** | **BPR=12.0, FN00=78.2 кN, electric system** |
|---|---|---|---|---|---|
| Drive type | conventional | conventional | conventional | conventional | electric. |
| BPR | 9.0 | 12.0 | 15.0 | 12.0 | 12.0 |
| FN00 | 78.2 | 78.2 | 78.2 | 90.0 | 78.2 |
| $d_{in}$, mm | 397.6 | 441.2 | 478.2 | 470.6 | 441.2 |
| $D_{in}$, mm | 1405.0 | 1559.0 | 1690.0 | 1663.0 | 1559.0 |
| $x_{fan}$, mm | 329.9 | 360.0 | 386.9 | 383.1 | 360.0 |
| $d_{fan}$, mm | 640.2 | 699.8 | 754.0 | 747.0 | 699.8 |
| $D_{fan}$, mm | 1405.0 | 1559.0 | 1690.0 | 1663.0 | 1559.0 |
| $S_{fan}$, m$^2$ | 0.88297 | 1.206967 | 1.514045 | 1.36769 | 1.206967 |
| $x_{core}$, mm | 1883.3 | 1978.8 | 2115.5 | 2099.4 | 1978.8 |
| $d_{core}$, mm | 488.2 | 520.6 | 508.6 | 555.2 | 520.6 |
| $D_{core}$, mm | 788.8 | 812.2 | 804.8 | 867.0 | 812.2 |
| $S_{core}$, m$^2$ | 0.19828 | 0.20494 | 0.21228 | 0.233624 | 0.20494 |
| BPR | 9.0 | 12.0 | 15.0 | 12.0 | 12.0 |
| FN00 | 78.2 | 78.2 | 78.2 | 90.0 | 78.2 |
| $P_{total\ core}$, Pa | 33857.0 | 32.1927 | 27.4445 | 32.2962 | 32.2062 |
| $T_{total\ core}$, K | 612.407 | 614.155 | 593.992 | 617.688 | 619.926 |
| $G_{core}$, kg/s | 9.93 | 9.41997 | 9.2339 | 10.8003 | 9.40236 |
| $P_{total\ fan}$, Pa | 50943.0 | 46.825 | 44.3514 | 47.1191 | 46.7412 |
| $T_{total\ fan}$, K | 276.974 | 269.89 | 266.614 | 270.403 | 269.738 |
| $G_{fan}$, kg/s | 95.96 | 122.149 | 155.726 | 139.483 | 121.962 |

Optimization of engine nacelle geometry has permitted to reduce the effective thrust losses of the engine by the value in the range 0.7-1.2% depending on the engine variant. In the case of the considered engines, it corresponds to 120-190 N of effective thrust. Then, Table 4 shows the main characteristics of the engines with designed variants of engine nacelles.

**Table 4. Main aerodynamic characteristics of the engines with designed variants of engine nacelles**

| Parameter | BPR=9.0, FN00=78.2 кN, conventional systems. | BPR=12.0, FN00=78.2 кN, conventional systems | BPR=15.0, FN00=78.2 кN, conventional systems | BPR=12.0, FN00=90.0 кN, conventional systems | BPR=12.0, FN00=78.2 кN, electric systems |
|---|---|---|---|---|---|
| $P_{id}$, N | 11708 | 11786 | 11165 | 13636 | 11726 |
| $P_x$, N | 12249 | 12276 | 11509 | 14295 | 12217 |
| $F_x$, N | 1338 | 1395 | 1329 | 1667 | 1396 |
| $P_{eff}$, N | 10911 | 10880 | 10180 | 12628 | 10821 |
| $C_x$ | 0.05631 | 0.04779 | 0.03877 | 0.05012 | 0.04783 |
| **$dP_{eff}$, %** | **6.81** | **7.68** | **8.82** | **7.40** | **7.72** |
| Inlet characteristics | | | | | |
| $G_{in}$, kg/s | 105.9 | 131.7 | 151.8 | 149.7 | 131.4 |
| *f* | 0.702 | 0.710 | 0.696 | 0.710 | 0.709 |
| *nu* | 0.998 | 0.997 | 0.998 | 0.998 | 0.997 |
| Nozzle characteristics | | | | | |
| $G_{id}$, kg/s | 108.8 | 135.1 | 157.1 | 153.9 | 152.9 |
| *G*, kg/s | 105.9 | 131.7 | 151.8 | 149.7 | 131.4 |
| $G_1$, kg/s | 8.8 | 8.3 | 4.3 | 9.3 | 8.3 |
| $G_2$, kg/s | 97.1 | 123.3 | 147.5 | 140.5 | 123.1 |
| *Cf8* | 0.9736 | 0.9744 | 0.9663 | 0.9725 | 0.9744 |
| *Cv9* | 1.0150 | 1.0116 | 1.0075 | 1.0137 | 1.0117 |
| *Cd9* | 0.9759 | 0.9762 | 0.9743 | 0.9772 | 0.9761 |
| $P_{id}$, N | 11708 | 11786 | 11165 | 13636 | 11726 |
| $P_x$, N | 12249 | 12276 | 11509 | 14295 | 12217 |
| $F_x$, N | 1338 | 1395 | 1329 | 1667 | 1396 |

Figure 24 shows the comparison of the optimal geometries for the same thrust engines and various bypass ratio BPR = 9, 12 and 15 (engine variants #1, 2 and 3). Table 3 shows the corresponding geometrical parameters. As it is obvious in the Figure, total engine nacelle length and its diameter increase with growing bypass ratio. It is connected, mainly, with growth of the engine size. The table shows that the inlet throat diameter, the diameter according to the leading edge and the midsection diameter grow proportionally to the engine entrance diameter. At the same time, the relative length of the outer lip of engine nacelle diminishes. According to growing the length of the outer contour nozzle edge, the degree of the nozzle efficiency increases, but the external drag grows too. The length of the outer contour nozzle lip is a compromise between the thrust losses in the nozzle and thrust losses associated with external drag. According to growing the engine diameter, external drag has an increasing important role, and the optimal relative length of the outer lip diminishes in spite of growing losses in the nozzle.

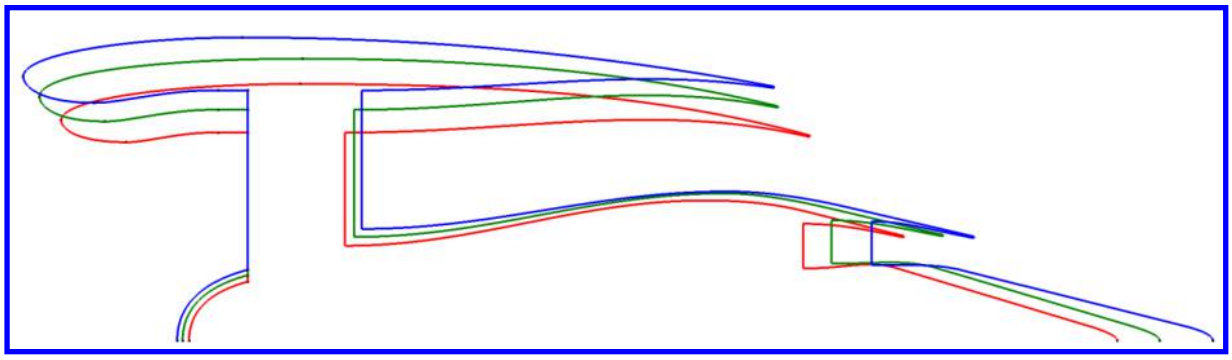

**Figure 24. Comparison of optimal engines with the same geometries and different bypass ratios: red color —BPR=9, green — BPR=12, blue — BPR=15**

The HI-FI CFD calculation for optimized full configuration have been performed. Once the geometric models of engine nacelles have been designed, their installation on the aircraft is performed. For that, a pylon position under the wing has been determined and a pylon for each variant of engine has been designed. Figure 25 shows the pressure coefficient distribution along the aircraft surface for isolated airframe and for 3 configuration variants. Table 5 presents the aerodynamic characteristics of the aircraft for the configuration with considered engines installed.

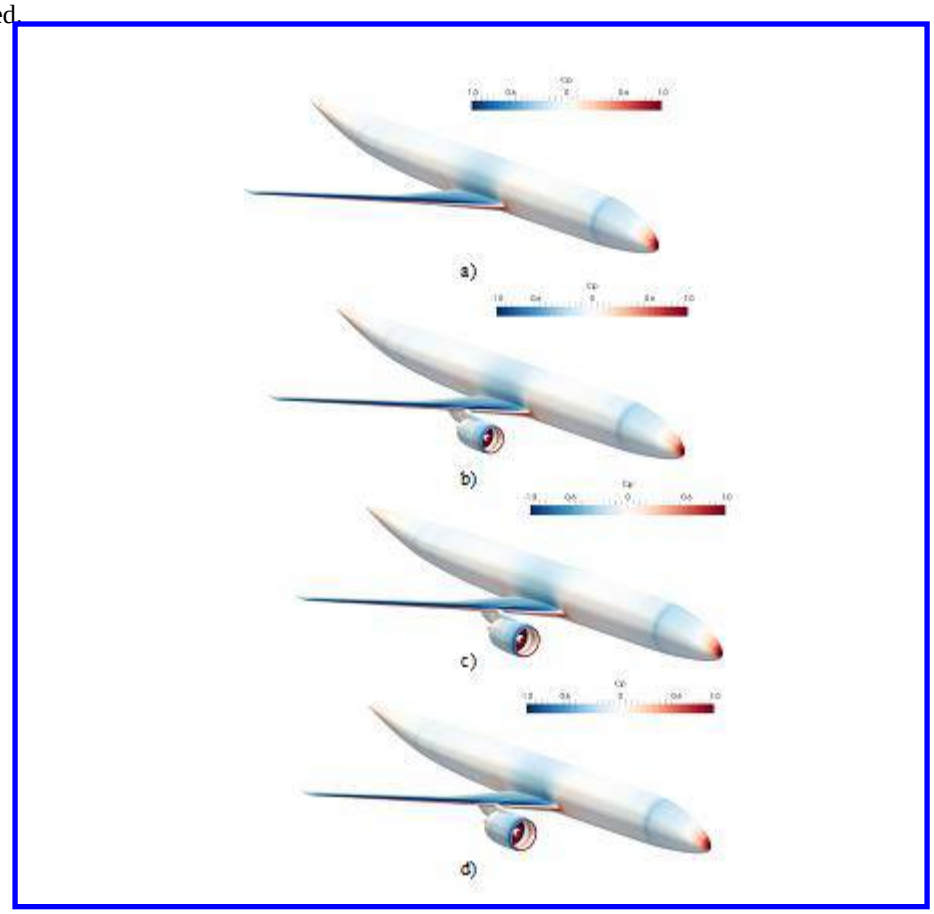


**Figure 25. The pressure coefficient distribution along the aircraft surface for the four engine variants: a) airframe without engine, b) engine with BPR=9, c) engine with BPR=12, d) engine with BPR=12 and with increased thrust**

**Table 5. Main aerodynamic characteristics of the engines with designed variants of engine nacelles**

| Parameter | Airframe without engine | BPR=9.0, FN00=78.2 κN, conventional. | BPR=12.0, FN00=78.2 κN, conventional. | BPR=12.0, FN00=90.0 κN, conventional. | BPR=12.0, FN00=78.2 κN, electric. |
|---|---|---|---|---|---|
| $P_x$, N | 0.0 | 12412 | 12261 | 14260 | 12201 |
| $F_x$, N | 9558 | 10047 | 9776 | 9839 | 9770 |
| $F_y$, N | 171317 | 158796 | 156989 | 153518 | 157019 |
| $C_x$ | 0.026344 | 0.027691 | 0.026945 | 0.027117 | 0.026928 |
| airframe | 0.026344 | 0.021719 | 0.021537 | 0.019909 | 0.021518 |
| engine nacelle drag | 0.0 | 0.004670 | 0.004360 | 0.006350 | 0.004366 |
| pylon | 0.0 | 0.001302 | 0.001048 | 0.000858 | 0.001044 |
| $C_y$ | 0.472184 | 0.437673 | 0.432692 | 0.423127 | 0.432775 |
| airframe | 0.472184 | 0.444787 | 0.440784 | 0.430601 | 0.440865 |
| engine nacelle | 0.0 | -0.007489 | -0.008749 | -0.008753 | -0.008749 |
| pylon | 0.0 | 0.000375 | 0.000657 | 0.001279 | 0.000659 |
| $C_y/C_x$ | 17.92 | 15.81 | 16.06 | 15.60 | 16.07 |

## 5. *Mission Simulation*

The below figures provides the result from DLR's mission simulation post infusion of all the results from different competencies (aero, structure, propulsion systems, nacelle drag ) for the given mission requirements.

Figure 26 represents the fuel consumption effect due to change in BPR of the engine, Conventional Aircraft system architecture and also the drag of Nacelle and weight of Nacelle considered. The BPR 12 seem to be optimum for the current fixed airframe. **BPR 9 consumes 5.6% more fuel compared to BPR 12 as per the evaluation**. Although BPR 15 is better in terms of SFC, the weight and drag leads to higher fuel consumption. Also the Landing gear weight for BPR 15 would be higher and heaver due to ground clearance issue. The detailed landing gear effect is not presented in the paper.

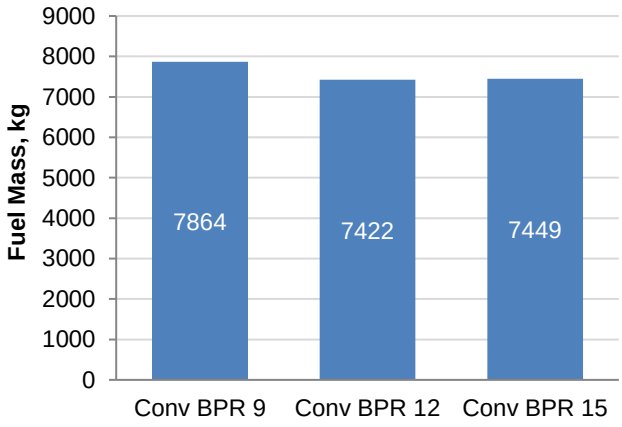


**Figure 26. Fuel Mass: BPR 9, 12 and 15 (Conventional Systems Architecture)**

Figure 27 presents effect of System architecture change in Fuel consumption. The comparison of Conventional, MEA 1, MEA 2 and AEA system architecture can be observed. This shows that the frame work can successffuly consider the effect of aircraft system offtake effects, propagate through changes in engine performance maps for each system architecture. The weights of systems, engine, pylon and drag of optimized Integrated Nacelle airframe is considred. But , it was realized that the offtake were not considered with coorect bleed power extraction assumption. Thus, this study was repeated with correct bleed extraction for MEA 1 and Conventional Arctecture.

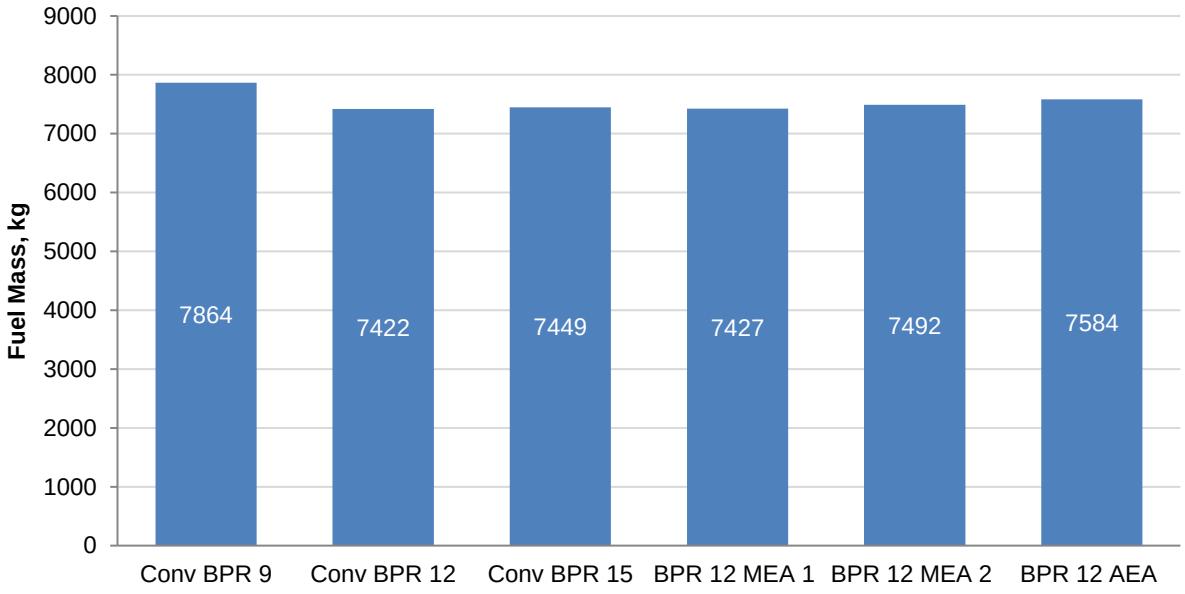


**Figure 27. Fuel consumption Results for System Architecture Variation**

After assuming correct offtake conditions the results were changed. The change is highlighted for One Aircraft system architecture in Figure 28. It can be observed that the BPR 12 conventional system architecture with corrected offtake assumptuion: consumes is 5.6% more fuel than earlier analysis with Incorrect offtake bleed assumption. This evaluation showed that detailed offtake bleed considerations is necessary for Aircraft Design Process, and in future this method is employed for MDO. Also the devil is in details seems true by this analysis. This study will be repeated for other system architecture which involves bleed. i.e BPR 12 for MEA 1 architecture. Thus, can be compared with all architectures; Conventional, MEA1, MEA2 and AEA for BPR 12. The Figure 28 will be updated by conference release.

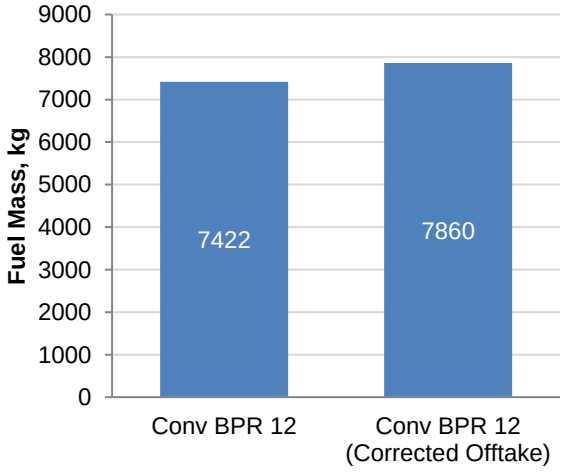


**Figure 28. Fuel Mass for BPR 12 vs BPR 12 corrected offtake (Conventional Systems Architecture)**

Now, the effects on Fuel consumption (Primary Objective Fuction) due to change in Airframe design, Aero , Structure, Engine , System and Nacelle were observed in this section.The other effects on emission and cost (Secondary Objectie) function would be presented in subsequent sections.

## 6. *Costs and Emissions*

The results of the cost and emission assessment carried out by RWTH Aachen were obtained using the output files provided after execution of the DLR mission analysis tool FSMS. The performed use case study follows a two-step approach. In the first step a study with a conventional aircraft systems architecture is carried out changing the bypass ratio (BPR) of the mounted engines from 9 to 12 and finally to 15 (BPR9, BPR12, and BPR15). The second step contains a more detailed evaluation on the BPR12 engine considering four different on-board systems architectures given in Table 6.

**Table 6. System architectures considered for assessment of costs and emissions**

| Engine name | Systems architecture | Engine BPR | Bleed offtakes | Hydr. system |
|---|---|---|---|---|
| BPR9_conv | Conventional | 9 | yes | yes |
| BPR12_conv | Conventional | 12 | yes | yes |
| BPR15_conv | Conventional | 15 | yes | yes |
| BPR12_MEA1 | More electric | 12 | yes | no |
| BPR12_MEA2 | More electric | 12 | no | yes |
| BPR12_AEA | All electric | 12 | no | no |

In the following, the study is first split into cost analysis and emission analysis. Finally, a combined assessment will be carried out with closer inspection of the operational phase. The focus is then set on the tradeoff between ecological and economic effects with the help the commonly used metrics Average Temperature Response (ATR) and Cash Operating Costs (COC).

**Cost Results:** The cost results for the comparison study of three different engine BPR (conventional on-board system architectures) are shown in Figure 29 including recurring costs (RC) on the left, and cash operating costs (COC) on the right hand side. The numbers are given in percentages with the BPR9 engine as a baseline.

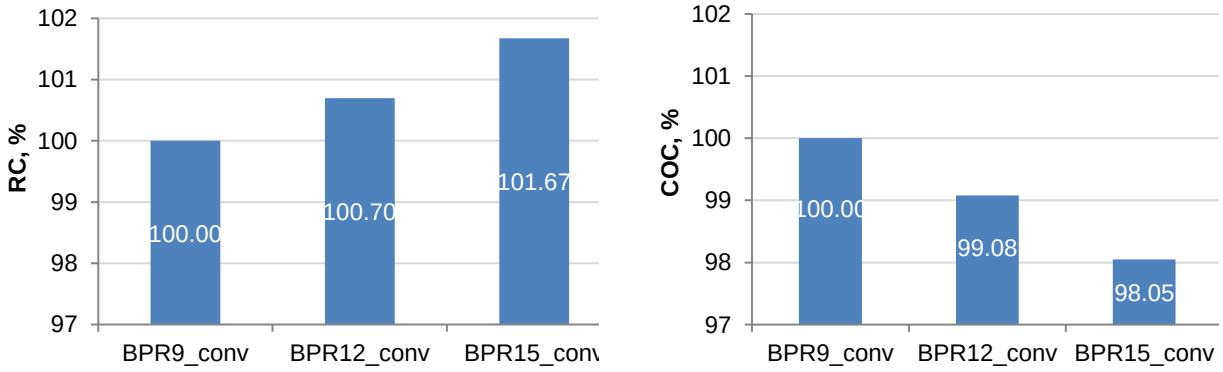


**i) Recurring Costs (RC)** **ii) Cash Operating Costs (COC)**

**Figure 29. RC and COC for three different engine BPR**

The figure shows that RC increase by about 0.7 % from BPR9 to BPR12 and again by about 1 % from BPR12 to BPR15. This is mainly caused by an increase in engine weight that results from the higher BPR. On the other hand, the COC (see Figure 29 ii) are decreased by almost 2 % from BPR9 to BPR15 due to the higher engine efficiency – and thus lower fuel burn on the mission – that comes with an increased BPR. As for the absolute cost numbers this means that the RC are overcompensated by the operational savings after one year of operations when moving from

BPR9 to BPR12, and after two years when moving from BPR12 to BPR15. Please note that these numbers apply taking into account a utilization of the aircraft of 1500 flights per year.

Proceeding with the more detailed analysis on the four different system architectures of the BPR12 engine, Figure 30 shows the change in RC in percentages with the conventional architecture (BPR12_conv) as a baseline.

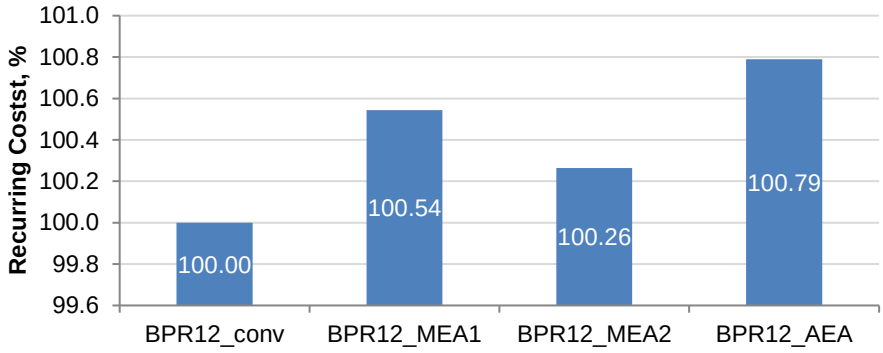


**Figure 30. RC for different system architectures (BPR12 engine)**

It can be seen, that the total change of RC is below 1 % (corresponds to approx. $ 20,000 in terms of absolute numbers) for all architectures. The reasons for the observed changes are diverse. MEA1 architecture for instance has no hydraulic system and therefore a relatively complex electrically driven flight control system that is more expensive than a conventional one. The all electric architecture (AEA) is the most expensive one, due to the complexity of the on-board systems that results from the full electrification.

Closer examination of the COC results (see Figure 31 ii) for the BPR12 studies show that the above described effect of higher RC for a larger amount of electrification is eliminated by the increased operational efficiency. The higher RC can be overcompensated by the decrease in COC after one year of operations when moving from the conventional to each of the more/all electric system architectures.

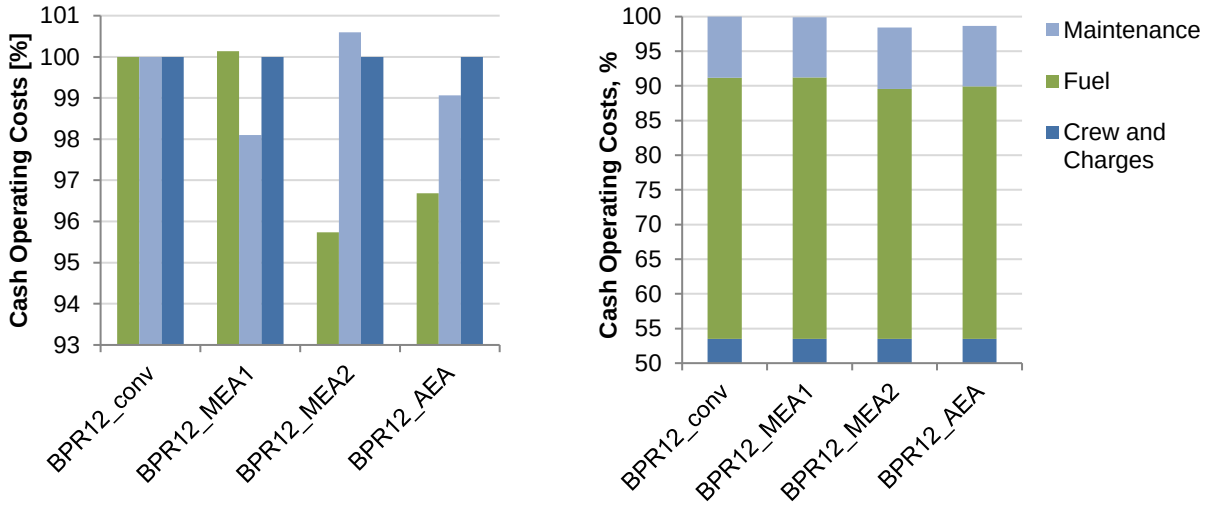


**i) Change in COC parts** **ii) Change in total COC**

**Figure 31. COC results for different on-board system architectures (BPR12 engine)**

MEA1 architecture has the lowest total COC of all on-board system architectures. This is directly proportional to the amount of fuel mass consumed during the mission, as can be seen from Figure 27. Costs for crew and charges (navigation, landing, ground handling) are constant, whereas maintenance and fuel costs vary over the different system architectures (see Figure 31 i). This shows that the amount of electrification also has an impact on maintenance expenses in the performed study. The MEA1 architecture leads to the lowest maintenance costs,

whereas MEA2 architecture even has a higher value than the conventional architecture. The reason for this is twofold. On the one hand, on the MEA1 the maintenance expensive hydraulic system was removed, while the conventional environmental control system remained. The AEA has a more complex architecture with electric environmental control system. On the other hand, on MEA2 the hydraulic system remained, while at the same time the environmental control system was electrified, leading to an increase in maintenance expenses on the electric system of the aircraft. Therefore, MEA1 architecture seems to be the most favorable architecture in terms of simplicity (maintenance) and efficiency (fuel burn). Please note that the above described cost effects result from the underlying cost models of the RWTH Aachen tools (described in section B6)and may vary when applying a different methodology.

**Emission Results:** In order to examine the effect of increased engine BPR on emissions the first step of the emission analysis within the scope of this paper is the observation of the emissions for the landing and takeoff (LTO) cycle of the three different engine BPR. From Figure 32 it can be observed that there is a significant reduction in emissions (13.6 % in total) from BPR9 to BPR15 while at the same time the rated thrust is increased by about 3.5 %.

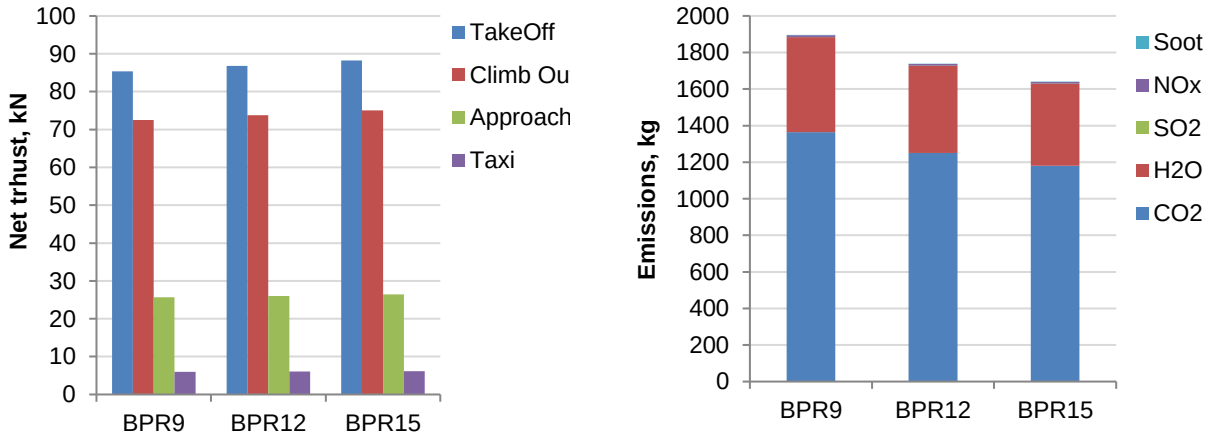


**Figure 32. Comparison of rated thrust and LTO emissions between the three different engine BPR**

From the BPR9 to BPR12 engine the reduction of emissions is about 8.4 % while at the same time net thrust is increased by 1.6 %.

On closer inspection of the four on-board system architectures on the BPR12 engine it becomes clear that, as expected, the change in exhaust of $CO_2$, $H_2O$, $SO_2$ and soot scales linearly with the amount of consumed fuel (see Figure 33). Note that the conventional architecture (BPR12_conv) was taken as baseline.

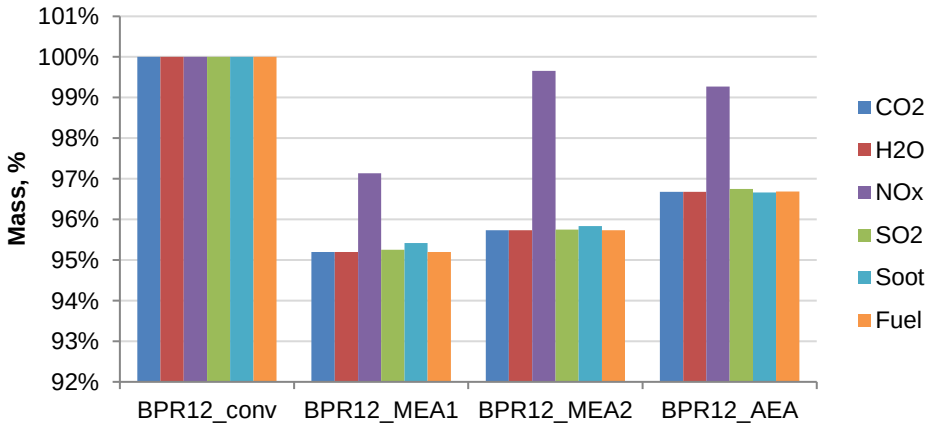


**Figure 33. Mass change for fuel and exhaust emissions**

However, the exhaust of $NO_x$ emissions is more complex and does not directly correlate with the fuel flow, but rather with the thermodynamic conditions of the engine in the current flight regime (e.g. pressure and temperature ratios at the entry of the combustion chamber). In short, it can be seen that the MEA1 architecture is the most favorable in terms of exhaust emissions. Despite these results, it should be mentioned that the impact on the environment resulting from these emissions does not simply scale with their amount, but also with the altitude in which they are emitted. It is therefore necessary to take a closer look at ecological metrics such as Average Temperature Response (ATR) in order to allow an assessment of ecological effects. This will be described in the following section combining the cost and emission analyses to an overall assessment of economic and ecological effects

**Economic and Ecological Assessment**

Figure 34 shows the relative change in COC in comparison to the relative change in ATR.

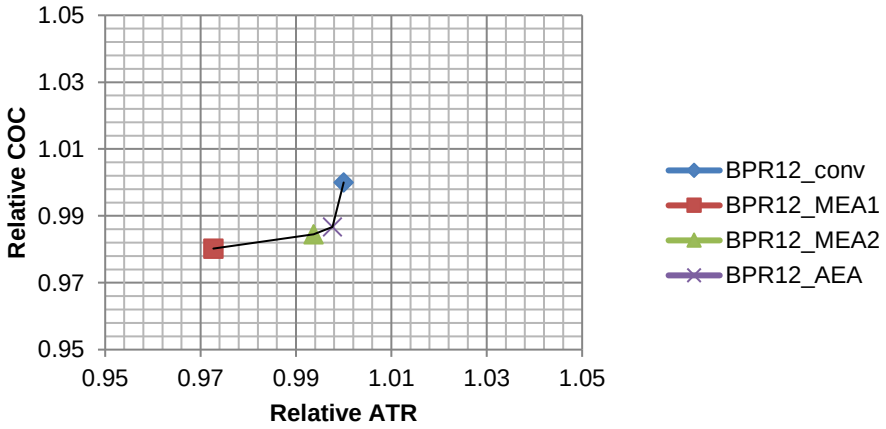


**Figure 34. Comparison between relative ATR and relative COC**

It can be observed that there are only slight deviations in ATR and COC (lower than 0.03 %) for the different on-board system architectures. As expected from the previous separated cost and emission analyses the results show that the more electric architecture MEA1 is the most favorable for consideration of both economic and ecological aspects.

## VI. Conclusion and Future Works

The collaborative SoS optimization approach (Figure 3)involving multiple partners, with multi-disciplinary tools hosted at different location was validated with a reference Test case aircraft (Figure 12). The analysis successfully propagated the effects of change in Engine BPR, Aircraft System Architecture's Degree of electrification changes, Nacelle optimization & Nacelle Aerodynamic Integration effects (Drag and Weight) and evaluated the fuel consumption: Figure 26, Figure 27, Figure 28 and Emission and Cost impacts : Figure 29 to Figure 34.

In summary the studies conducted for System of Systems framework for AGILE reference Aircraft and results:

1) Varying BPR : Figure 26 , Shows that BPR 12 is the optimum
2) Varying Architecture : Figure 27, Shows More Electric 1 Combination for BPR 12 is optimum
3) Offtake Effects are mapped and relative change in fuel due to correct offtake assumption: Figure 28 shows corrected offtake would lead to upto 5.6% higher fuel consumption
4) Cost Modeling for the different combination of Engine BPR and Systems : Figure 29 to Figure 31 shows Higher BPR is efficient in terms of Cost(without considering Landing gear effect on 15 BPR). MEA1 architecture seems to be the most favorable architecture in terms of simplicity (maintenance) and efficiency (fuel burn).
5) Emission Modeling for engines and aircraft system combination : Figure 32 and Figure 33 shows emission reduction with BPR (efficiency) and MEA 1 seems efficient.
6) Economic and Eological Assessment for the System of Systems study : Figure 34 shows MEA 1 system architecture combination with BOR 12 is most optimum.

The sensitivity and coupling of local design and global variables are provided shows the success of MDO framework. Future work would include, evaluating the framework for Multi-Fidelity of same disciplines. Response surface methods for time efficiency would be considered. Secondly,testing the robustness of analysis modules and frame work for 5 more conventional and unconventional AGILE reference configurations. New MDO strategies would be considered.

## Acknowledgments

Authors would like to thank all partners of AGILE consortium (www.agile project.eu) and European Union for the support. This project has received funding from the European Union Horizon 2020 Programme (H2020-MG-2014-2015) under grant agreement n◦ 636202. TsAGI revived funding for this project from The Ministry of Education and Science of the Russian Federatio- framework agreement No. 14.628.21.0004 (Project unique identifier RFMEFI62815X0004).Special thanks to WP 3 Task Leader Thierry Lefebvre of ONERA who led this MDO work package 3, DLR's Jonas Jepsen for continued CPACS support and AIAA MDO TC and AIAA for hosting AGILE session.

## References

[1] P. D. Ciampa and B. Nagel, "Towards the 3rd generation MDO collaboration Environment," in 30th Congress of the International Council of the Aeronautical Sciences, Daejeon, 2016.

[2] AGILE Paradigm: developing the next generation collaborative MDO," in 18th AIAA\ISSMO Multidisciplinary Analysis and Optimization Conference, Denver, 2017

[3] I. van Gent, P. D. Ciampa, B. Aigner, J. Jepsen, G. La Rocca and J. Schut, "Knowledge Architecture supporting collaborative MDO in the AGILE paradigm," Conference, 2017.in 18th AIAA\ISSMO Multidisciplinary Analysis and Optimization

[4] Ciampa, P. D., Baalbergen, E. H., and Lombardi, R., "A Collaborative Architecture supporting AGILE Design of Complex Aeronautics Products," 18th AIAA/ISSMO Multidisciplinary Analysis and Optimization Conference, 2017.

[5] Lefebvre, T., Bartoli, N., Dubreuil, S., Panzeri, M., Lombardi, R., Della Vecchia, P., Nicolosi, F., Ciampa, P. D., Anisimov, K., and Savelyev, A., "Methodological enhancements in MDO process investigated in the AGILE European project,"
18th AIAA/ISSMO Multidisciplinary Analysis and Optimization Conference, 2017.

[6] Zill, Thomas, Pier Davide Ciampa, and Björn Nagel. "Multidisciplinary design optimization in a collaborative distributed aircraft design system." 50th AIAA Aerospace Sciences Meeting. 2012

[7] Pier Davide Ciampa, T. Zill, and Bjoern Nagel. "Aeroelastic Design and Optimization of Unconventional Aircraft Configurations in a Distributed Design Environment", 53rd AIAA/ASME/ASCE/AHS/ASC Structures, Structural Dynamics and Materials Conference Co-located Conferences,2012

[8] Chiesa, Sergio, Giovanni Antonio Di Meo, Marco Fioriti, Giovanni Medici, and Nicole Viola. " Aircraft on board systems sizing and trade-off analysis in initial design." (2012): 1-28.

[9] Fioriti, M., Boggero, L., Corpino, S., Isyanov, A., Mirzoyan, A., Lombardi, R., D'Ippolito, R., "Automated Selection of the Optimal On-board Systems Architecture within MDO Collaborative Environment", AIAA Aviation 2017, 5-9 June, Denver, USA

[10] Neyland, V. Ya., Bosnyakov, S. M., Glazkov, S. A., Ivanov, A. I., Matyash, S. V., Mikhailov, S. V., and Vlasenko, V. V., "Conception of electronic wind tunnel and first results of its implementation," Progress in Aerospace Sciences, Vol. 37, No. 2, 2001, pp. 121-145.

[11] Anisimov, K. S. and Savelyev, A. A., "Aerodynamic Optimization of Airplane Propulsion System within the Framework of AGILE Project," 30 th ICAS Congress, Daejeon, Korea, September 2016.

[12] Franz, K., Lammering, T., Risse, K., Anton, E., and Hoernschemeyer, R., "Economics of Laminar Aircraft Considering Off-Design Performance," 53rd AIAA/ASME/ASCE/AHS/ASC Structures, Structural Dynamics and Materials Conference & 20th AIAA/ASME/AHS Adaptive Structures Conference, American Institute of Aeronautics and Astronautics, Reston, Virigina, 2012.

[13] Lammering, T., Franz, K., Risse, K., Hoernschemeyer, R., and Stumpf, E., "Aircraft Cost Model for Preliminary Design Synthesis," 50th AIAA Aerospace Sciences Meeting including the New Horizons Forum and Aerospace Exposition, American Institute of Aeronautics and Astronautics, Reston, Virigina, 2012.

[14] Intergovernmental Panel on Climate Change, "IPCC Special Report - Aviation and the Global Atmosphere," 1999.

[15] Dallara, E. S., Kroo, I. M., and Waitz, I. A., "Metric for Comparing Lifetime average Climate Impact of Aircraft," AIAA Journal, Vol. 49, No. 8, 2011, pp. 1600–1613

[16] Franz, K., Risse, K., and Stumpf, E., "Framework for Sustainability-Driven Aircraft Design," 2013 Aviation Technology, Integration, and Operations Conference, American Institute of Aeronautics and Astronautics, Reston, Virginia, 2013.